co2amp 2020

Mikhail Polyanskiy

January 5, 2023

Contents

Chapter 1

General notes

1.1 Program capabilities

1. Ultrashort pulse amplification in CO_2 active medium
   - Rotational numbers up to $J = 60$
   - Regular, hot and sequence bands
   - Isotopic CO_2
2. Molecular dynamics
   - Realistic pumping
   - Collisional relaxation processes
   - Stimulated transitions
   - Independent consideration of active medium regions at different elongations from the optical axis
3. Diffraction-based beam propagation
   - Beam manipulation with common optical elements
   - Arbitrary optical configurations
4. Linear dispersion and non-linear effects in optical materials
   - Pulse chirping
   - Kerr lensing
   - Self-phase modulation
5. Advanced optics
   - Chirped-pulse amplification
   - Spectral filtering
   - Trains of pulses
   - Staging (program output as an input for the next stage)
6. User's interface
   - Easy specification of parameters
   - Graphical output
   - Project save/recall

1.2 Availability, tools and third party components

The simulation core **co2amp** and the user's interface shell **co2am+** are written in C++ programming language. **co2am+** uses the QT library (`http://qt.io`), and QT Creator (a part of the QT project) is used as a development environment. Windows executables are built using the MinGW compiler obtained as a part of the open-source QT distribution. The code is published in the GitHub website (`https://github.com/polyanskiy/co2amp`) and is freely available for use, modification, and redistribution under the terms of the GNU General Public License (GPL v.3) (`https://www.gnu.org/licenses/gpl-3.0.html`). A binary package is provided in the form of a Windows installer that contains pre-compiled executables, documentation, templates and examples at `https://github.com/polyanskiy/co2amp/releases/`. The project only uses cross-platform libraries and thus should compile under other platforms (MacOS, Linux). **co2amp** depends on three third party components: gnuplot, 7-zip and HDF5 that are freely available for multiple platforms at `http://www.gnuplot.info/`, `https://www.7-zip.org/` and `https://www.hdfgroup.org/solutions/hdf5/` respectively. These components must be installed separately. The windows installer is built using the Nullsoft Scriptable Install System (NSIS, `https://nsis.sourceforge.io/`), and this is the only platform-specific part of the project. Finally, the documentation is mostly written in LaTeX(http://www.latex-project.org) using the Overleaf online editor and compiler (`https://www.overleaf.com/`). YAML and HDF5 file formats are adopted for the specification of input parameters and storing the output field information respectively.

1.3 Acknowledgements

Viktor Platonenko from Moscow State University (Russia) provided a `Mathcad` code for pulse amplification in the CO_2 active medium that was used as the starting point for developing the `co2amp` program; Dr. Platonenko also offered valuable input in the early stages of the work.

Chapter 2

Basic concepts

2.1 co2amp and co2am+

co2amp is a terminal program that allows simulating propagation of ultrashort pulses through an arbitrary cylindrically-symmetric optical system that can include CO_2 amplifiers. It takes inputs in the form of specially formatted text files and command line arguments and produces outputs in the form of tabulated data files and a binary file with the complete information on the output field. **co2amp** can be used independently, however a graphical user interface makes the task of managing the program's inputs and outputs much more convenient.

co2am+ is a graphical user interface program that simplifies the process of working with multiple input- and output- files and calculation parameters by keeping them organized and easily accessible via an intuitive working environment. **co2am+** allows saving/recalling the entire file structure of a project and command line parameters in a single compressed '.co2' file.

2.2 Projects

The **co2amp** input parameters include the characteristics of the initial `pulse(s)`, the optical `layout` configuration, specifications for all `optics` used in the model (including laser amplifiers), and calculation parameters (e.g. calculation grid definition).

The temporal shape of the pulse and the beam profile at every element of the optical layout are saved and can be accessed in both graphical and tabulated-numerical representations.

All **co2amp** inputs and outputs for a certain model constitute a project.

co2am+ allows storing all inputs and outputs of the model except the output field in a single compressed project file with a '.co2' extension. Complete pulse information (complex field in every node of the space-time calculation grid) at the output of the system can be saved separately as a binary HDF5 file ('.pulse' extension) and used as an input for another project. An example of the input file structure of a '.co2' project accessed via the **co2am+** interface is shown in Fig. 2.1.

2.3 `Pulse`, `layout` and `optic`

A `pulse` is a complex electric field defined in every node of the calculation grid. A project can include one or more input pulses. Each one of them is defined in a separate YAML ('.yml') file. Either a reference to an output from another project (a '.pulse' file) or an explicit specification of the pulse's spatial- and temporal-profile can be used to define an input pulse.

The optical `layout` consists of a series of infinitely-thin `optics` separated by free space. `Pulses` propagate freely between the `optic`. A project must have one and only one `layout`. The `layout` is defined in a '.yml'

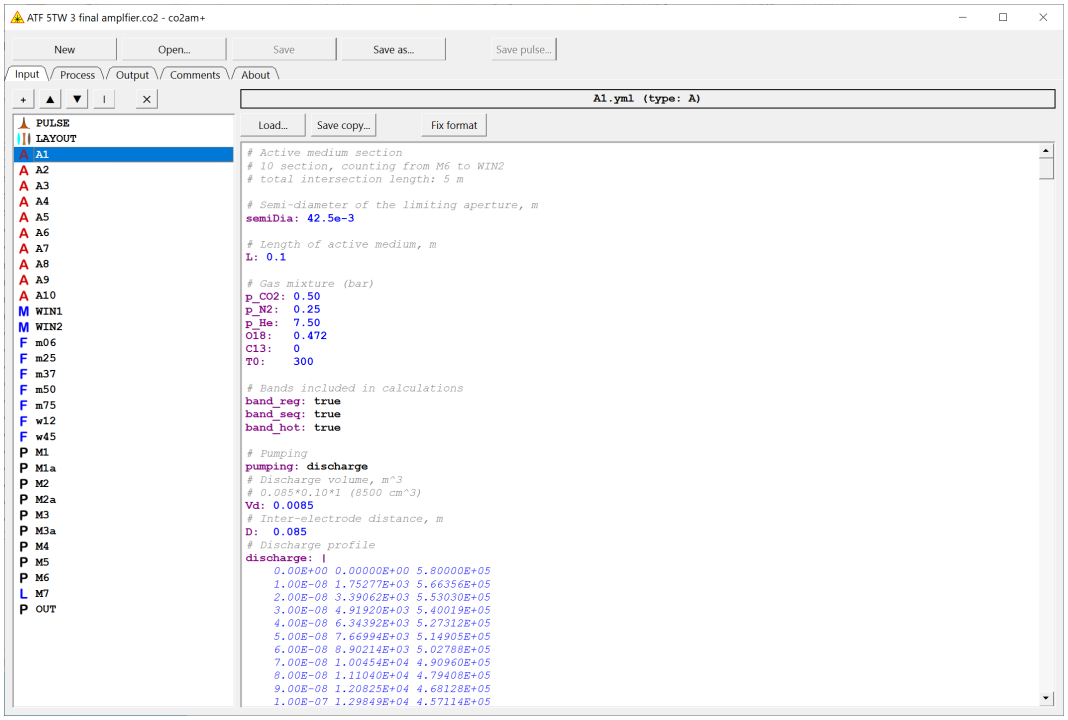

Figure 2.1: "Input" tab of the **co2am+** user interface program. YAML files specifying the `pulse`, `layout` and `optics` are listed on the left. Content of a selected file is displayed and can be edited in the big edit box on the right.

file that specifies the order of the `planes` and distances between them.

An `optic` is an element of a system that alters the pulse when it passes through it. There are several types of `optic` described in some detail later. For example, a *Lens* is an `optic` that introduces a radial-coordinate-dependent frequency shift changing the divergence of the beam. Each `optic` is specified in a separate '.yml' file. One `optic` can be used several times in the same `layout`. In this case `pulses` pass through the `optic` several times as, for example, in a laser cavity[1].

co2amp supports seven types of `optics` listed in the Table 2.1

2.4 Calculation grid

The `pulse` is defined as a complex electric field in the nodes of a 2-dimensional space-time calculation grid moving with the pulse. Calculation grid is mostly defined via **co2amp** command line arguments. The only exception is the maximum radial coordinate that is equal to the semi-diameter of the clear aperture of an `optic` and thus changes from `optic` to `optic`. The command line arguments associated with the pulse space-time calculation grid are the numbers of nodes ("precision") in the pulse time- and radial coordinate-grids, minimum- and maximum- time limits and the central frequency. The central frequency is needed to unambiguously define the calculation grid in the frequency domains.

Pulse time frame is used for all `pulse` related calculations (interaction with `optics`, free-space propagation) and for fast processes in some `optics`, e.g. fast molecular dynamics (stimulated transitions and rotational relaxation in an *Active medium*). Processes that are much slower than the duration of the pulse

[1]Internally, **co2amp** code uses an additional concept: a `plane`. A `plane` is an element of a `layout` that, unlike an `optic`, only appears in the `layout` once. An `optic` is then associated with each `plane`. A `plane` is basically a placeholder for an `optic`.

Table 2.1: Types of `optics`

Type ID	*Name*	*Description*
A	*Active medium*	A CO_2 amplifier section.
P	*Probe*	A passive surface. May be used as a limiting aperture.
F	*Spatial filter*	An `optic` with coordinate-dependent transmission.
S	*Spectral filter*	An `optic` with frequency-dependent transmission.
L	*Lens*	An ideal thin lens.
M	*Material*	A layer of a material. May introduce linear- and/or non-linear dispersion and/or absorption.
C	*Chirper*	An `optic` that applies a chirp to the pulse. Typically stretcher or compressor.

(e.g. pumping of the active medium and vibrational relaxation) are modeled separately in a slower laboratory time-frame. Time-tick of the laboratory time-frame is also defined via a **co2amp** command line argument.

In **co2am+** the **co2amp** command line arguments are specified in the "Process" tab (Fig. 2.2). The number of nodes in both coordinates of the pulse space-time frame always is a power of two that allows the use of Fast Fourier Transform (FFT) algorithms. Calculations with a larger number of nodes usually are more accurate but, on the other hand, take longer and require more computer memory (both calculation time and required memory are roughly proportional to the product of the number of nodes in the time and space grids). Therefore it is recommended to start running the simulation with a smaller number of nodes and then repeat it several times, each time with a denser grid. The absence of considerable change in the program's output with an increase in the number of nodes will indicate that the density of the grid is satisfactory.

The time-step, $\Delta t = (t_{max} - t_{min})/N_t$, where t_{max} and t_{min} define the time range and N_t is the number of nodes in the time grid, must be small enough to accurately describe the pulse profile at all stages of its propagation through the optical system. It also is important to remember that the time range and number of nodes in the time grid also define the range and step in the frequency domain: $\Delta\nu = 1/(t_{max} - t_{min})$ and $(\nu_{max} - \nu_{min}) = 1/\Delta t$. This means that the time range must be long enough to provide sufficient resolution in the frequency domain, while, concurrently, the time step must be sufficiently short to provide a bandwidth that fits the entire spectral region of interest.

Identifying an appropriate calculation grid is very important for building an accurate model of an optical system. Putting an effort in this part of the simulation process will pay off with fast, reliable calculations.

2.5 Units

SI units without prefixes, e.g. "meters, seconds, Amperes..." but not "centimeters, nanoseconds, kiloamperes...", are used in **co2amp** input and output and also in the **co2amp** code internally. **co2amp+** allows changing the units used for the graphical representation of the calculation results on the "Output" tab (Fig. 2.3). However, when numerical data are accessed via [Right-click on a plot] – [Copy raw data] the units of the data are always "prefix-less".

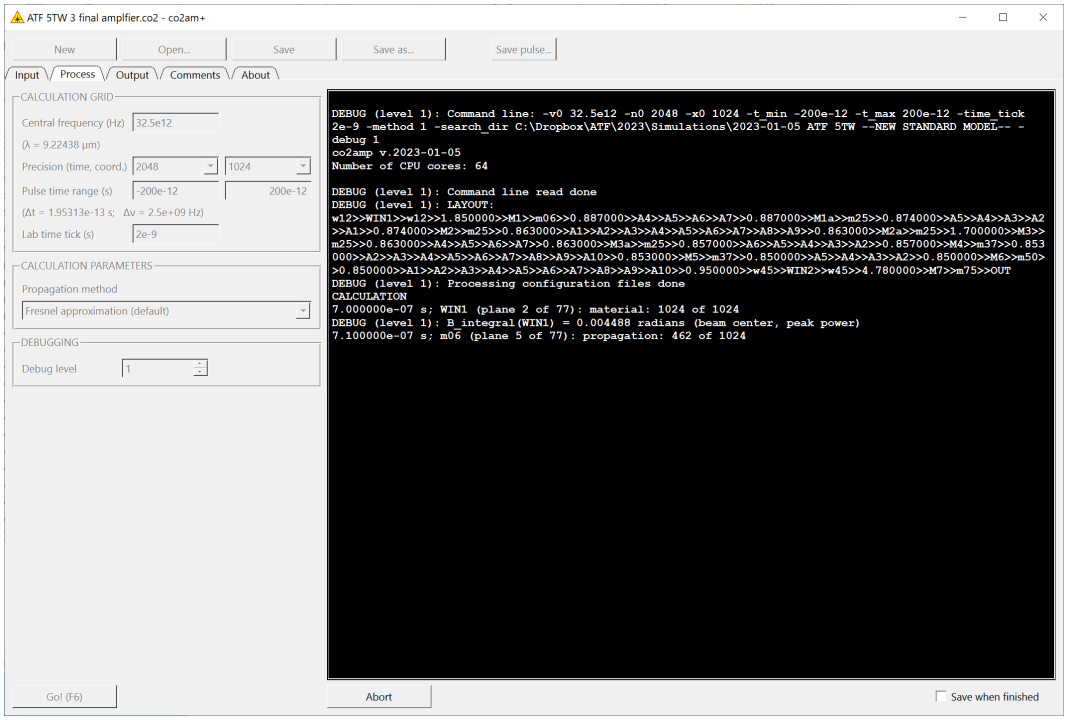

Figure 2.2: "Process" tab of the **co2am+** user interface program. Values of **co2amp** command line arguments are specified on the left. **co2amp** output is displayed in the black text box on the right.

2.6 Program output

The output of the program is given as a temporal and spatial structure of every `pulse` at each `optic` in the `layout`. Temporal (and spectral) profiles are integrated on the entire area of the `optic`, and spatial profiles are integrated on the duration of the pulse time-frame.

In the **co2am+** "Output" tab the user can chose a `pulse` and an `optic` to display (Fig. 2.3). If the selected `optic` is used several times in the `layout`, it also is possible to specify which passes through the `optic` will be displayed. Also, the integral pulse energy can be provided either at every pass through a selected `optic`, or at all passes through all `optics` of the `layout`.

Output for some types of `optics` supplies additional type-specific information. For instance, for *Active medium*, this includes gain, discharge profile, population dynamics, and the dynamics of the distribution of pumping energy (fractions of discharge energy going into the excitation of laser levels, excitation of molecular translations and ionization). Output for the optic of type *Probe* include the information of the phase of the optical field in the center of the beam.

2.7 "Comments" and "About" tabs of co2am+

The "Comments" tab provides an edit box to enter any comments about the project that will be stored as a part of the project in the '.co2' file.

The "About" tab contains information about the versions of the **co2amp** and **co2am+** programs, links to the license and the documentation (this file), author contact information, and a suggested citation format.

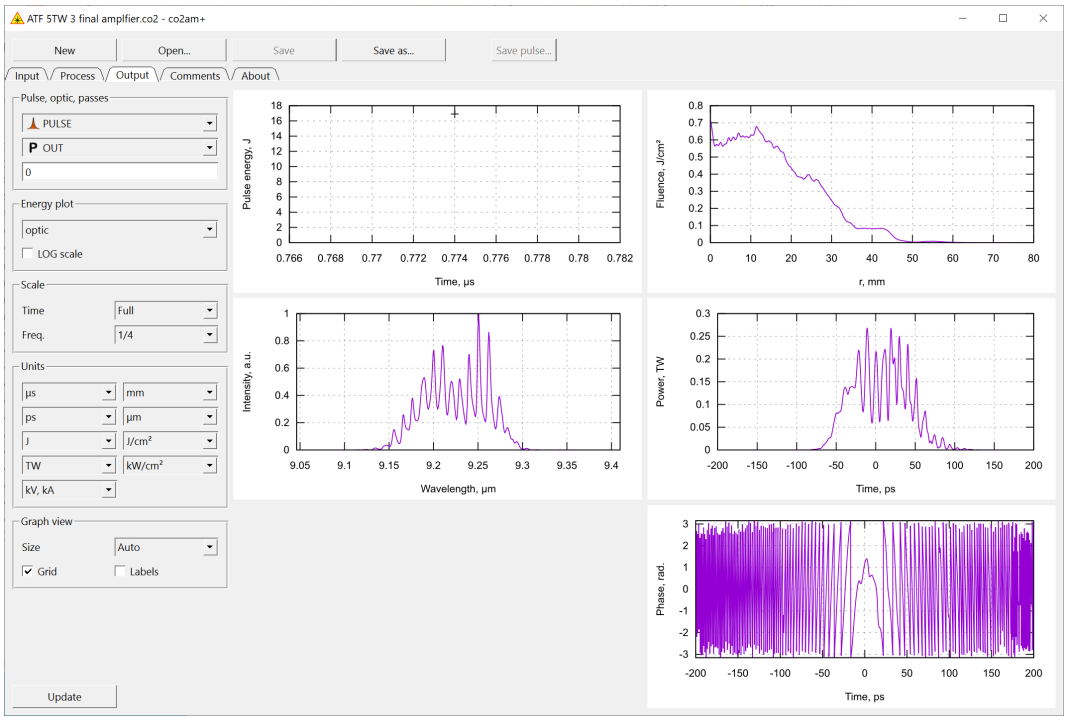

Figure 2.3: "Output" tab of the **co2am+** user interface program. Controls on the left allow selecting the data to display and fine-tuning the look of the plots.

Chapter 3

Elements of a project

A project must include the following elements specified in the input YAML files:

1. One or more `pulses`
2. One or more `optics`
3. One `layout`

Each element is specified in a dedicated YAML ('.yml') file[1]. The last `optic` in the `layout` must be of type P (*Probe*).

In the following sections we briefly describe each of these elements and discuss models associated with them. This description is not complete. Refer to the templates and the example files (and the comments in them) for more information.

3.1 `Pulse`

Unless the output of another project ('.pulse' file) is used as an input, both the temporal- and spatial- shape of the input `pulse` must be specified in a corresponding YAML ('.yml') file. The `pulse` is assumed to be transform-limited (no initial chirping). The `pulse` energy, central frequency, and the injection time must also be specified. The injection time specifies the time-delay between the zero moment of the lab time frame ("slow" time frame) and injecting a `pulse` into the optical system (first `optic` in the `layout`). An example of a `pulse` configuration file is shown below.

```
#========================
# PULSE.yml from 'examples/00 simple propagation.co2' project

t_in: 0
E: 1e-3
freq: 32.5e12

beam: GAUSS
w: 3e-3

pulse: GAUSS
fwhm: 2e-12
#========================
```

[1] **co2amp** also requires an additional input file 'config_files.yml' that lists all input YAML files and the types of corresponding elements. **co2am+** creates this file automatically.

This file specifies a 2 ps (FWHM) transform-limited Gaussian pulse with an $w = 3$ mm Gaussian beam profile, 1 mJ energy and 32.5 THz central frequency injected into the system at $t_{in} = 0$. There are several pre-defined beam- and pule- profile options: `GAUSS`, `FLATTOP`, `SUPERGAUSS4`, `SUPERGAUSS6` etc. Alternatively, a `FREEFORM` option can be selected followed by a tabulated numerical specification of an arbitrary shape (see 'pulse.yml' template for details).

3.2 Layout

3.2.1 Configuration

The `layout` configuration defines the order of `optics` and the distances between them. A simple `layout` configuration file looks like this:

```
#=========================
# LAYOUT.yml from 'examples/00 simple propagation.co2' project

- go: P1 >> 3 >> P2
  times: 1
#=========================
```

Here, the system consists of two `optics`: `P1` and `P2` separated by 3 meters of free space. The pulse(s) pass through the system once. If the `times` value is more than 1, a pulse after passing through `P2` will go to `P1` again, and the propagation through the system will repeat the specified number of times. There can be several "go-times" in a `layout` configuration file. An example of a `layout` configuration for a more complex system is shown below

```
#=========================
# LAYOUT.yml from 'examples/ATF 5 TW/ATF 1 regen.co2' project

- go: str >> COU1
  times: 1

- go: 0.45 >> i >> 0.90 >> GE >> 0.25 >> w >> WIN1 >> w >> 0.45 >> AM1 >> 0.40 >> AM2 >> 0.45
>> w >> WIN2 >> w >> 0.10 >> MIR >> m >> 0.10 >> w >> WIN2 >> w >> 0.45 >> AM2 >> 0.40 >> AM1
>> 0.45 >> w >> WIN1 >> w >> 0.25 >> GE >> 0.90 >> i >> 0.45 >> COU2
  times: 15

- go: 0.45 >> i >> 0.90 >> GE >> 0.25 >> w >> WIN1 >> w >> 0.45 >> AM1 >> 0.40 >> AM2 >> 0.45
>> w >> WIN2 >> w >> 0.10 >> MIR >> m >> 0.10 >> w >> WIN2 >> w >> 0.45 >> AM2 >> 0.40 >> AM1
>> 0.45 >> w >> WIN1 >> w >> 0.25 >> OUT
  times: 1
  #=========================
```

3.2.2 Dealing with long optical elements

In the **co2amp** model, the `optics` are infinitely thin. In a case of a long `optic`, for example an *Active medium*, the model first calculates the field modification accumulated by a `pulse` when it propagates through the `optic` and then apply it as if it occurred at once. This approach may not work well if the actual optical element is long and the `pulse` changes considerably while propagating through it, thus interacting differently with different parts of the `optic`. Accuracy of the model can be improved if long elements are divided into shorter sub-sections.

Fig. 3.1 shows an example of a 2-meter long `layout` with a meter long active medium in the middle. In one case shown in Fig. 3.1a we first propagate the`pulse` to the middle of the amplifier section, then apply the amplification accumulated over 1 meter and propagate the`pulse` to the last `optic`. The corresponding

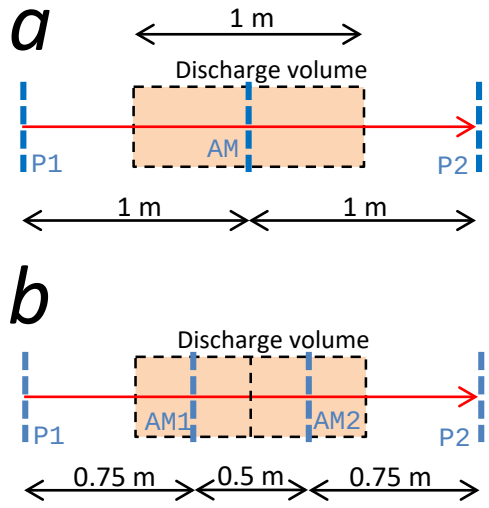

Figure 3.1: Example of `layout` configuration for a long `optic` (in this case an *Active medium*. a) The *Active medium* is represented by a single `optic`. b) The *Active medium* is split in two shorter sections.

`layout` configuration is

```
#=========================
# long amplifier

- go: P1 >> 1 >> AM >> 1 >> P2
  times: 1
#=========================
```

Alternatively, we can represent the active medium by two 0.5-meter sections as shown in Fig. 3.1b. The corresponding layout is

```
#=========================
# long amplifier is divided in two shorter sections

- go: P1 >> 0.75 >> AM1 >> 0.5 >> AM2 >> 0.75 >> P2
  times: 1
#=========================
```

Population dynamics in all amplifier sections is modeled separately, and thus, by splitting a long amplifier into shorter sections we also obtain a more realistic model of the active medium.

3.2.3 Modelling of `pulse` propagation between `optics`

Consider free-space wave propagation between plane-parallel surfaces S' and S separated by distance z as shown in Fig. 3.2 for the case of cylindrical symmetry. According to Huygens-Fresnel principle, the field E in a point on the plane S is defined as a superposition of secondary waves emitted from every point of plane

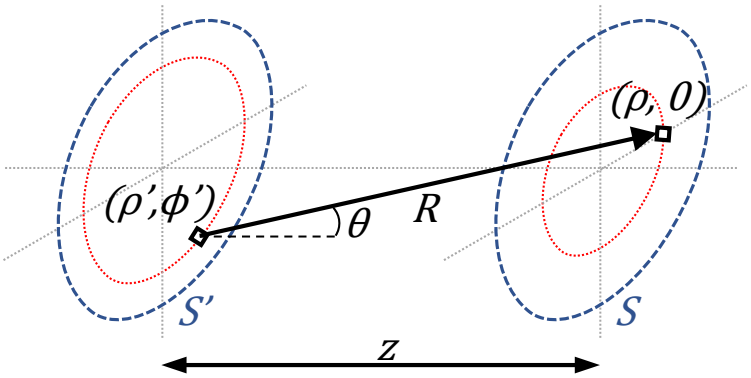

Figure 3.2: Application of Huygens-Fresnel principle to beam propagation from plane S' to plane S for a system with cylindrical symmetry.

S' [1]. This can be written in the case of cylindrical symmetry as [2, 3]

$$E(\rho) = -\frac{i}{\lambda}\int_{\rho'=0}^{\infty} E'(\rho')\int_{\phi'=0}^{2\pi}\frac{e^{ikR}}{R}K d\phi'\rho' d\rho' \tag{3.1a}$$

$$R = \sqrt{\rho^2 + \rho'^2 + z^2 - 2\rho\rho'\cos\phi'} \tag{3.1b}$$

$$K = \cos\theta = \frac{z}{R} \tag{3.1c}$$

where λ is the wavelength, $k = 2\pi/\lambda$ the wavenumber, and K the obliquity factor as it appears in Rayleigh-Sommerfeld diffraction theory.

Note that because the field on the output plane S doesn't depend on the angular coordinate ϕ, $\phi = 0$ is chosen for the simplification of Eq. (3.1).

Direct numerical integration of Eq. (3.1) having $O(N^3)$ complexity is very time consuming and thus an approximation is usually used to accelerate computations. Fresnel diffraction is the most known approximation to the diffraction integral. The following assumptions are done in the Fresnel approximation

$$\begin{aligned} K &\approx 1 \\ R &\approx \begin{cases} z & \text{(denominator)} \\ z\left(1 + \frac{\rho^2+\rho'^2-2\rho\rho'\cos\phi'}{2z^2}\right) & \text{(exponent)} \end{cases} \end{aligned} \tag{3.2}$$

where "denominator" and "exponent" signify the position of the R variable in Eq. (3.1a).

After substituting Eq. (3.2) to Eq. (3.1a) and using the following formula

$$\int_0^{2\pi} e^{\pm ia\cos\phi} d\phi = 2\pi J_0(a) \tag{3.3}$$

where J is the Bessel function we get the expression for Fresnel diffraction with cylindrical symmetry

$$E(\rho) \approx -\frac{2\pi i e^{ik\left(z+\frac{k\rho^2}{2z}\right)}}{\lambda z}\int_0^{\infty} E'(\rho')e^{i\frac{k\rho'^2}{2z}} J_0\left(\frac{k\rho\rho'}{z}\right)\rho' d\rho' \tag{3.4}$$

co2amp supports both Rayleigh-Sommerfeld- Eq. (3.1) and Fresnel- Eq. (3.4) based propagation methods. Also, the user can chose to ignore the `pulse` evolution during free-space propagation.

Eq. (3.1) and Eq. (3.4) assume a monochromatic light, which is not the case for ultrashort pulses that have non-negligible bandwidth. Therefore, in **co2amp** the propagation is calculated in frequency domain: Eq. (3.1) or Eq. (3.4) are applied to Fourier-transformed field in every node of the frequency calculation grid. After that an inverse Fourier transform is used to return to the time domain.

3.3 `Optic` type A *Active medium*

Active medium is by far the most complex `optics` that can be used in a **co2amp** project. The models used for simulating the molecular dynamics and `pulse` amplification are described in a dedicated Chapter 4.

Configuration file for an `optic` of type A must include specifications of the gas mixture, pumping, and laser transitions included in the simulations. An example of a configuration file is shown below

```
#=========================
# AM1.yml from 'examples/ATF 5 TW/ATF 3 final ampifier.co2' project

# Semi-diameter of the limiting aperture, m
semiDia: 45e-3

# Length of active medium, m
L: 0.57

# Gas mixture (bar)
p_CO2: 0.50
p_N2:  0.25
p_He:  7.50
O18:   0.472
C13:   0
T0:    300

# Bands included in calculations
band_reg: true
band_seq: true
band_hot: true

# Pumping
pumping: discharge
# Discharge volume, m^3
Vd: 0.0085
# Inter-electrode distance, m
D:  0.085
# Discharge profile
discharge: |
    0.00E+00 0.00000E+00 5.80000E+05
    1.00E-08 1.97186E+03 5.66356E+05
    2.00E-08 3.81445E+03 5.53030E+05
    3.00E-08 5.53410E+03 5.40019E+05
    4.00E-08 7.13691E+03 5.27312E+05
    ...
#=========================
```

The composition (including isotopic enrichment of carbon dioxide) and the initial temperature of the active medium are specified under the "#Gas mixture (bar)" comment.

For discharge pumping, the geometry of the discharge and its profile must be given. For optical pumping, the wavelength, the absorption cross-section, and the temporal profile of the pumping pulse must be provided.

Comments in the 'optic A (discharge pumped CO2 amplifier).yml' and
'optic A (optically pumped CO2 amplifier).yml' template files provide a detailed information on the format of the configuration file.

3.4 `Optic` type P *Probe*

Probe is a passive `optic`. It doesn't change the field that fits inside its semi-diameter.

$$E(t,\rho) = E'(t,\rho) \tag{3.5}$$

where $E'(t,\rho)$ and $E(t,\rho)$ is the field before- and after- an `optic` respectively.

However, a *Probe* `optic` can be used as a limiting aperture that has a zero transmittance for $\rho > semiDia$. The only configuration parameter for an `optic` of type P is its semi-diameter. A configuration file for a 25 mm semi-diameter *Probe* is shown below

```
#=========================
# probe

semiDia: 25e-3
#=========================
```

3.5 `Optic` type F *Spatial filter*

Spatial filter applies a specified coordinate-dependent transmittance function to a `pulse`

$$E(t,\rho) = E'(t,\rho)\sqrt{\mathcal{T}(\rho)} \tag{3.6}$$

where $\mathcal{T}(\rho)$ is the transmittance function defined in the configuration file.

Configuration example:

```
#=========================
# spatial filter

semiDia: 25e-3

filter: SIN
r_min: 10e-3
#=========================
```

See the 'optic F (spatial filter).yml' template file for details

3.6 `Optic` type S *Spectral filter*

Spectral filter applies a specified frequency-dependent transmittance function to a `pulse`

$$\begin{aligned} \widehat{E}'(\nu,\rho) &= \mathcal{F}(E'(t,\rho)) \\ \widehat{E}(\nu,\rho) &= \widehat{E}'(\nu,\rho)\sqrt{\mathcal{T}(\nu)} \\ E(t,\rho) &= \mathcal{F}^{-1}(\widehat{E}(\nu,\rho)) \end{aligned} \tag{3.7}$$

where $\mathcal{F}$ and $\mathcal{F}^{-1}$ are the Fourier transform and the inverse Fourier transform respectively, ν is the frequency, and $\mathcal{T}(\nu)$ is the transmittance function defined in the configuration file.

Configuration example:

```
#========================
# spectral filter

semiDia: 25e-3

filter: FREEFORM
form: |
    32.0e12 1.0
    32.1e12 0.9
    32.2e12 0.7
    32.3e12 0.5
    32.4e12 0.3
    32.5e12 0.0
    32.6e12 0.3
    32.7e12 0.5
    32.8e12 0.7
    32.9e12 0.9
    33.0e12 1.0
#========================
```

See the 'optic S (spectral filter).yml' template file for details

3.7 `Optic` type L *Lens*

Lens is a lens.

$$\begin{aligned} \widehat{E}'(\nu,\rho) &= \mathcal{F}(E'(t,\rho)) \\ \widehat{E}(\nu,\rho) &= \widehat{E}'(\nu,\rho)\exp\left(-\frac{ik\rho^2}{2F}\right) \\ E(t,\rho) &= \mathcal{F}^{-1}(\widehat{E}(\nu,\rho)) \end{aligned} \tag{3.8}$$

where $k = \frac{2\pi\nu}{c}$ is the wave number (c is the speed of light) and F is the focal length of the lens.

The calculation is done in frequency domain to ensure that effective focal length is same for all frequencies in the pulse spectrum.

Configuration example (1-meter focal length lens):

```
#========================
# lens (F = 1 m)

semiDia: 25e-3

F: 1.0
#========================
```

3.8 `Optic` type M *Material*

In the case of an oblique incidence, effective intensity I_{eff} is reduced and propagation distance in the material (effective thickness) Θ_{eff} is increased automatically depending on the incidence angle θ_i and the refractive

index n of the material

$$\begin{aligned}\theta_r &= \arcsin\left(\frac{\sin\theta_i}{n_0}\right)\\ I_{eff} &= I\frac{\cos\theta_i}{\cos\theta_r}\\ \Theta_{eff} &= \frac{\Theta}{\cos\theta_r}\end{aligned} \tag{3.9}$$

where I and Θ are the intensity before the `optic` and the actual thickness of the material and θ_r is the refraction angle.

Linear dispersion and absorption

$$\begin{aligned}\widehat{E}'(\nu,\rho) &= \mathcal{F}(E'(t,\rho))\\ \widehat{E}(\nu,\rho) &= \widehat{E}'(\nu,\rho)\exp(2\pi i\Delta\nu)\sqrt{\exp(-\alpha_0\Theta_{eff})}\\ E(t,\rho) &= \mathcal{F}^{-1}(\widehat{E}(\nu,\rho))\end{aligned} \tag{3.10}$$

where

$$\Delta\nu = \int_0^{\nu}(\nu'-\nu_c)\frac{dt}{d\nu'}d\nu', \tag{3.11}$$

c is the speed of light,

$$\frac{dt}{d\nu'} = \frac{\Theta_{eff}}{c}\frac{dn_g}{d\nu'}, \tag{3.12}$$

ν_c is the central frequency.

where $\widehat{E}(\nu,\rho)$ is the field in the frequency domain, $\mathcal{F}$ and $\mathcal{F}^{-1}$ are the Fourier-transform and inverse-Fourier-transform functions, ν is the frequency, ν_c is the central frequency, n_g is the group index of refraction. The dispersion formulas used for calculating n_g are given in Appendix C.

Nonlinear interaction

$$\begin{aligned}E(t,\rho) &= E'(t,\rho)\exp\left(2\pi i\nu_c\frac{\Theta_{eff}}{c}n_2 I_{eff}(t,\rho)\right)\\ I_{eff}(t,\rho) &= 2h\nu_c(E'(t,\rho))^2\frac{\cos\theta_i}{\cos\theta_r}\end{aligned} \tag{3.13}$$

where n_2 is the nonlinear refractive index, h the Plank's constant, and $I(t,r)$ is the field intensity. The numerical values of n_2 used in the program are given in Appendix C.

Configuration example:

```
#=========================
# material

semiDia: 25e-3

material:  NaCl
thickness: 100e-3
tilt: 0
slices: 10
#=========================
```

The following materials are currently supported: CdTe, GaAs, Ge, KCl, NaCl, Si, ZnSe, and air. An arbitrary n_2 can be specified in the configuration file. A pre-defied value (Appendix C) is used otherwise. To improve accuracy, the *Material* `optic` can be split in several layers. A split-step method is used to calculate linear- and non-linear interaction with a layer: first, a non-linear interaction with a half-layer is calculated, then a full-layer linear interaction, and finally a half-layer nonlinear interaction again.

3.9 `Optic` type C *Chirper*

Chirper introduces a chirp to a pulse and is typically used to model a stretcher or compressor.

$$\begin{aligned} \widehat{E}'(\nu,\rho) &= \mathcal{F}(E'(t,\rho)) \\ \widehat{E}(\nu,\rho) &= \widehat{E}'(\nu,\rho)\exp(2\pi i\Delta\nu) \\ E(t,\rho) &= \mathcal{F}^{-1}(\widehat{E}(\nu,\rho)) \end{aligned} \tag{3.14}$$

where

$$\Delta\nu = \int_0^{\nu} (\nu' - \nu_c)\frac{dt}{d\nu'}d\nu', \tag{3.15}$$

ν_c is the central frequency, and $\frac{d\nu}{dt}$ is chirpyness.

In the case of linear chirp the chirpyness is constant and and Eq. (3.15) becomes

$$\begin{aligned} \Delta\nu &= \int_0^{\nu} \frac{\nu' - \nu_c}{\mathcal{C}}d\nu' = \frac{(\nu-\nu_c)^2}{2\mathcal{C}} \\ \mathcal{C} &= \frac{d\nu}{dt} \end{aligned} \tag{3.16}$$

Configuration example:

```
#========================
# stretcher (positive chirpyness => red chirp)

semiDia: 25e-3

chirp: LINEAR
c: 3.5e21
#========================
```

Only linear chirp is presently supported.

Chapter 4

Modelling of processes in CO_2 amplifiers

4.1 Molecular dynamics

Simulations of active medium pumping by electric discharge and vibrational relaxation are done following Karlov and Konev [4].

4.1.1 Pumping by electric discharge

Pumping is described by the Boltzmann equation in the following form [5, 6]:

$$-\frac{1}{3}\left(\frac{\mathcal{E}}{\mathcal{N}}\right)^2 \frac{d}{du}\left[u\left(\sum_j y_j Q_{mj}(u)\right)^{-1}\frac{df(u)}{du}\right] = 1.09\times10^{-3}\frac{d}{du}\left[u^2 f(u)\sum_j \frac{y_j}{M_j}Q_{mj}(u)\right] + \sum_{j=1,2} y_j C_j \frac{d}{du}(uf(u)) + 6By_2\frac{d}{du}(uQ(u)f) + \sum_j y_j \sum_k (u+u_{jk})Q_{jk}(u+u_{jk})f(u+u_{jk}) - uf(u)\sum_j y_j \sum_k Q_{jk}(u) \quad (4.1)$$

where the left part describes the energy of electrons in the electric field, the first component of the sum of the right part represents energy transfer via elastic collisions between electrons and molecules, the second and third components describe collisions with molecular rotation excitation, and the two last components relate to inelastic collisions with transfer of the energy u_{jk} into vibrational and electronic excitations and ionization.

Electron energy u is expressed in eV;

Ratio of the electric field to the full molecular density, $\mathcal{E}/\mathcal{N}$, is expressed in units of 10^{-16} V·cm^2;

y_j are the relative molecule concentrations ($j = 1$ corresponds to CO_2, $j = 2$ to N_2 and $j = 3$ to He);

$M_1 = 44$, $M_2 = 28$, $M_3 = 4$ are the molar masses;

$C_1 = 8.2\times10^{-4}$ eV·Å^2 [7];

$C_2 = 5.06\times10^{-4}$ eV·Å^2 [8];

$B = 2.5\times10^{-4}$ eV is the N_2 rotational constant.

Numerical values of the cross-sections Q and the transferred energies u_{jk} are summarized in Appendix A

Equation 4.1 is solved numerically using the tridiagonal matrix algorithm. Distribution function $f(u)$ is then used in the following calculations.

The rate constant ω_{jk}, and the electron drift speeds v_d are defined as:

$$\omega_{jk}\left[\frac{\mathrm{cm}^3}{\mathrm{s}}\right] = 5.93\times10^{-9}\int\limits_0^\infty uQ_{jk}(u)f(u)du \tag{4.2}$$

$$v_d\left[\frac{\mathrm{cm}}{\mathrm{s}}\right] = -5.93\times10^{7}\left(\frac{1}{3}\frac{\mathcal{E}}{\mathcal{N}}\right)\frac{df(u)}{du}\int\limits_0^\infty u\left(\sum_j y_jQ_{mj}(u)\right)^{-1}du \tag{4.3}$$

The fraction of electron energy transmitted via inelastic processes is defined as

$$z_{jk} = 10^{16}\frac{y_ju_{jk}\omega_{jk}}{\left(\frac{\mathcal{E}}{\mathcal{N}}\right)v_d} \tag{4.4}$$

The fraction of electron energy transmitted to translations and rotations are the following:

$$z_t = 5.93\times10^{7}\frac{1.09\times10^{-3}\int\limits_0^\infty u^2\left(\sum\limits_j\frac{y_j}{M_j}Q_{mj}(u)\right)f(u)du}{\left(\frac{\mathcal{E}}{\mathcal{N}}\right)v_d} \tag{4.5}$$

$$z_r = 5.93\times10^{7}\frac{\sum\limits_{j=1,2}y_jC_j\int\limits_0^\infty uf(u)du + 6y_2B\int\limits_0^\infty uQ(u)f(u)du}{\left(\frac{\mathcal{E}}{\mathcal{N}}\right)v_d} \tag{4.6}$$

Finally, the distribution of the excitation energy is calculated using the following expressions:
$q_2 = \sum\limits_{k=1}^{6} z_{1k}$ - fraction of energy transferred to CO_2 symmetric stretch (ν_1) and bending (ν_2) modes;
$q_3 = z_{17}$ - fraction of energy transferred to CO_2 asymmetric stretch mode (ν_3);
$q_4 = \sum\limits_{k=1}^{8} z_{2k}$ - fraction of energy transferred to N_2 vibrations;
$q_T = z_t + z_r$ - fraction of energy transferred to translation and rotation;
$q_{ei} = \sum\limits_{k=9}^{15} z_{2k} + \sum\limits_{k=8}^{10} z_{1k}$ - fraction of energy spent on excitation of electronic levels and ionization.

4.1.2 Pumping and vibrational relaxation dynamics

A 3-temperature model is used for describing the vibrational dynamics of the active medium of CO_2 amplifiers. In this model, the following temperatures are used to describe the distribution of the energy between molecular vibrations:

T_2 – vibrational temperature of ν_1 and ν_2 vibrations of CO_2;
T_3 – vibrational temperature of the ν_3 vibration of CO_2;
T_4 – vibrational temperature of N_2.

Vibrational temperatures are related to the average numbers of quanta e_x in the corresponding vibrations as follows:

$$\begin{aligned} e_2 &= \frac{2}{\exp(960/T_2)-1} \\ e_3 &= \frac{1}{\exp(3380/T_3)-1} \\ e_4 &= \frac{1}{\exp(3350/T_4)-1} \end{aligned} \tag{4.7}$$

"2" in the first equation is due to 2-fold degeneracy of the energy levels of the bend vibration.

The dynamics of pumping/relaxation is described by the following equations

$$\begin{aligned}\frac{de_4}{dt} &= p_{e4} - r_a(e_4 - e_3)\\ \frac{de_3}{dt} &= p_{e3} + r_c(e_4 - e_3) - r_3 f_3\\ \frac{de_2}{dt} &= f_2\left(p_{e2} + 3r_3 f_3 - r_2(e_2 - e_{2T})\right)\end{aligned} \tag{4.8}$$

where

$$\begin{aligned}&p_{e4} = 0.8\times10^{-3}\frac{q_4}{ny_2}W(t);\quad p_{e3} = 0.8\times10^{-3}\frac{q_3}{ny_1}W(t);\quad p_{e2} = 2.8\times10^{-3}\frac{q_2}{ny_1}W(t);\\ &f_2 = \frac{2(1+e_2)^2}{2+6e_2+3{e_2}^2};\quad f_3 = e_3(1+e_2/2)^3 - (1+e_3)(e_2/2)^3\exp(-500/T);\\ &r_a = kny_1;\quad r_c = kny_2;\quad r_2 = k_2 n;\quad r_3 = k_3 n;\\ &k_2 = \sum_{i=1}^{3} y_i k_{2i};\quad k_3 = \sum_{i=1}^{3} y_i k_{3i};\\ &n = 273\frac{p[\text{bar}]}{T_0[\text{K}]};\\ &e_{2T} = \frac{2}{\exp(960/T)-1}\end{aligned} \tag{4.9}$$

where $W(t)$ is the discharge power density measured in kW/cm^3 , p_e is measured in μs^{-1}, and the constants k are calculated using the following expressions [9, 10]:

$$\begin{aligned}&k = 240/T^{1/2};\\ &k_{31} = A(t)\exp(4.138 + 7.945x - 631.24x^2 + 2239x^3);\\ &k_{32} = A(t)\exp(-1.863 + 213.3x - 2796.2x^2 + 9001.9x^3);\\ &k_{33} = A(t)\exp(-3.276 + 291.4x - 3831.8x^2 + 12688x^3);\\ &k_{21} = 1.16\times10^3\exp(-59.3x);\\ &k_{22} = 8.55\times10^2\exp(-69x);\\ &k_{23} = 1.3\times10^3\exp(-40.6x)\end{aligned} \tag{4.10}$$

where $x = T^{-1/3}$, $A(t) = (T/273)(1+e_{2T}/2)^{-3}$, and temperature T is expressed in K.

Finally, the dynamics of the gas temperature is described by the following equation:

$$\frac{dT}{dt} = \frac{y_1}{C_V}(500r_3 f_3 + 960r_2(e_2 - e_{2T})) + 2.7\frac{W(t)q_T}{nC_V}, \tag{4.11}$$

where $C_V = 2.5(y_1 + y_2) + 1.5y_3$.

4.1.3 Optical pumping

In the case of optical pumping population dynamics is modelled with equations 4.7–4.11 with the exception of the expressions for excitation rates in Eq. 4.9 that are replaced by

$$\begin{aligned}&p_{e4} = 0;\\ &p_{e3} = \Phi\sigma;\\ &p_{e2} = \begin{cases} 0 & \textit{direct excitation of } (00^01) \textit{ at } \sim 4.3\ \mu m\\ 2\Phi\sigma & \textit{excitation via } (10^01, 02^01) \textit{ at } \sim 2.8\ \mu m\\ 4\Phi\sigma & \textit{excitation via } (20^01, 12^01, 04^01) \textit{ at } \sim 2.0\ \mu m\end{cases}\end{aligned} \tag{4.12}$$

where Φ is the flux of the pumping photons (number of photons per m^2 per second), and σ is the absorption cross-section. Equations 4.12 imply that each pumping photon delivers one quantum of energy to the upper laser level, and zero, two or four quanta to the lower level, depending on the pumping transition.

4.2 Amplification

4.2.1 Laser transitions

Fig. 4.1 shows the vibrational levels and laser transitions included in the `co2amp` amplification model (because of the lack of the spectroscopic data, the sequence and hot bands currently are only supported for natural isotopologue of CO_2 (626[1]).

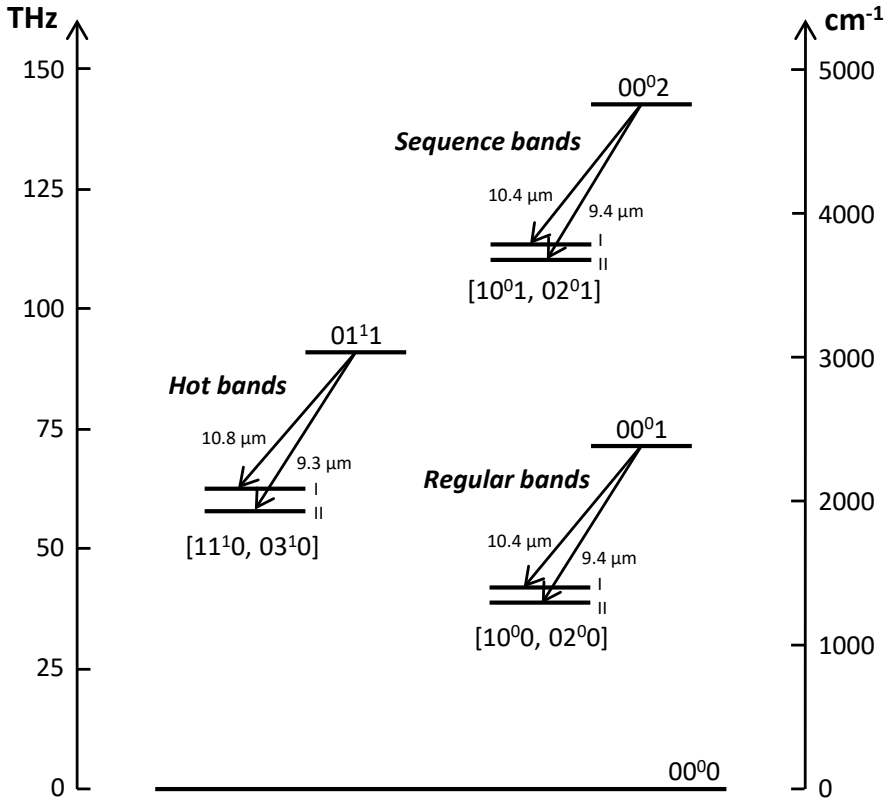

Figure 4.1: Vibrational transitions included in the amplification model. Wavelengths are given for natural CO_2 isotopologue (626).

4.2.2 Main equations

Amplification is simulated in the fast time-frame moving with the pulse using the following equations that also take into account rotational relaxation [11, 12]:

[1] A 3-digit notation commonly is used for designating the isotopologues (molecules with different isotopic composition) of carbon dioxide. In this notation *2*, *3* and *4* correspondingly stand for ^{12}C, ^{13}C and ^{14}C; *6*, *7* and *8* represent correspondingly ^{16}O, ^{17}O and ^{18}O. *626* denotes a CO_2 molecule with natural isotopic composition: ^{16}O-^{12}C-^{16}O.

$$\begin{aligned}
&\frac{\partial E}{\partial z} = -\sum_J \rho_J, \\
&\frac{\partial \rho_J}{\partial t} + \left(2\pi i(\nu_c - \nu_{0J}) + \frac{1}{\tau_2}\right)\rho_J = -\frac{\sigma_J n_J E}{2\tau_2}, \\
&\frac{\partial n_J}{\partial t} + \frac{n_J - n_J^0}{\tau_R} = 4(\rho_J E^* + c.c.),
\end{aligned} \tag{4.13}$$

where summation is done over all rotational-vibrational transitions of all CO_2 isotopologues, and

E - complex field envelope,

ρ_J - polarization of the medium,

z - linear coordinate along the direction of beam propagation,

t - time,

n_J - population inversion of the transition (difference of population densities of upper and lower levels),

n_J^0 - equilibrium population inversion of the transition,

ν_c - carrier frequency,

ν_{0J} - transition frequency in the line center,

σ_J - transition cross-section in the line center,

τ_2 - polarization dephasing time,

τ_R - rotational relaxation time.

Transition frequencies of P and R transitions are calculated as follows:

$$\nu_J = \begin{cases} V + B_U(J-1)J - B_L J(J+1) & (P) \\ V + B_U(J+1)(J+2) - B_L J(J+1) & (R) \end{cases} \tag{4.14}$$

where J is the rotational quantum number, V is the vibrational constant of the corresponding transition, and, B_U and B_L the rotational constants of the upper and lower level of the transition correspondingly. The numerical values of the molecular constants used in the program are listed in Appendix B.

The transition cross-section in the line center is calculated [13]

$$\sigma_J[\mathrm{m}^2] = \frac{(\lambda_J[\mathrm{m}])^2 A_J[\mathrm{s}^{-1}]}{4} \times \frac{\tau_2[\mathrm{s}]}{\pi} \tag{4.15}$$

where the first term defines the integral cross-section of the rotational line, and the second term is the maximum of the normalized Lorentzian profile of a line with width $2\pi\Delta\nu_{HWHM} = 1/\tau_2$.

Population inversion in the rotational equilibrium is calculated as

$$n_J^0 = \begin{cases} z(J-1)N_U - z(J)N_L & (P) \\ z(J+1)N_U - z(J)N_L & (R) \end{cases} \tag{4.16}$$

where N_U and N_L are the population densities of the corresponding upper and lower *vibrational* levels, and $z(J)$ is the Boltzmann distribution:

$$z(J) = \begin{cases} 2\dfrac{hB}{kT}(2J+1)\exp\left(-\dfrac{hB}{kT}J(J+1)\right) & (626, 636, 828, 838) \\ \dfrac{hB}{kT}(2J+1)\exp\left(-\dfrac{hB}{kT}J(J+1)\right) & (628, 638) \end{cases} \tag{4.17}$$

where $h = 6.62606957 \times 10^{-34}$ J·s and $k = 1.3806488 \times 10^{-23}$ J/K

Optical intensity I is related to the field amplitude as follows:

$$I[\mathrm{W/m}^2] = 2h[\mathrm{J{\cdot}s}]\nu_c[\mathrm{s}^{-1}]|E|^2 \tag{4.18}$$

Dephasing and relaxation times are defined by the following equations:

$$\begin{aligned}\tau_2[\mathrm{s}] &= \frac{10^{-6}}{\pi \times 7.61 \times 750 \times (P_{CO2} + 0.733P_{N2} + 0.64P_{He})} \\ \tau_R[\mathrm{s}] &= \frac{10^{-7}}{750 \times (1.3P_{CO2} + 1.2P_{N2} + 0.6P_{He})}\end{aligned} \tag{4.19}$$

where pressure P is measured in bars.

4.2.3 Populations

In the approximation used in the `co2amp` model, the processes of pumping and vibrational relaxation are slow compared to the duration of the pulse. Thus, only the stimulated transitions contribute to the change of the populations of vibrational levels during the pulse.

In the fast time-frame associated with the pulse there is no equilibrium in the vibrational energy distribution, and a proper population dynamics rather than the temperature model must be used. Thus, during the amplification, population of each rotational-vibrational level is considered independently. After the pulse leaves the active medium, the energy distribution within each vibrational mode becomes normalized quickly, and can be described by the temperature model again.

An important simplification used in the model is the assumption that vibrational temperatures T_2 and T_3 are the same for all CO_2 isotopologues. This assumption can be justified by the relatively small energy mismatch between vibrational levels of different isotopic species of the same molecule, and thus, fast inter-molecular V-V energy exchange. However, this assumption may not hold if the time-delay between two consecutive passes of a pulse through the amplifier is short compared to the relaxation times of intra-mode and inter-isotopic vibrational energy.

Initial populations of vibrational levels are calculated for each isotopologue and for each band using the following equations:

Regular band

$$N_{00^01} = \frac{N}{\mathcal{Q}} \exp\left(\frac{-3380}{T_3}\right)$$

$$N_{[10^00,02^00]_I} = N_{[10^00,02^00]_{II}} = \frac{N}{\mathcal{Q}} \exp\left(\frac{-2 \times 960}{T_2}\right)$$

Sequence band

$$N_{00^02} = \frac{N}{\mathcal{Q}} \exp\left(\frac{-2 \times 3380}{T_3}\right)$$

$$N_{[10^01,02^01]_I} = N_{[10^01,02^01]_{II}} = \frac{N}{\mathcal{Q}} \exp\left(\frac{-2 \times 960}{T_2}\right) \exp\left(\frac{-3380}{T_3}\right)$$

Hot band

$$N_{01^11} = \frac{N}{\mathcal{Q}} \exp\left(\frac{-3380}{T_3}\right) \exp\left(\frac{-960}{T_2}\right)$$

$$N_{[11^10,03^10]_I} = N_{[11^10,03^10]_{II}} = \frac{N}{\mathcal{Q}} \exp\left(\frac{-3 \times 960}{T_2}\right)$$

(4.20)

where N is the density of CO_2 molecules, and $\mathcal{Q}$ the partition function [14]:

$$\frac{1}{\mathcal{Q}} = \left(1 - \exp\left(\frac{-1920}{T_2}\right)\right) \times \left(1 - \exp\left(\frac{-3380}{T_3}\right)\right) \times \left(1 - \exp\left(\frac{-960}{T_2}\right)\right)^2 \tag{4.21}$$

Change of the populations in the regular band due to stimulated transitions is calculated for each vibrational level using the last of the equations 4.13:

$$\begin{aligned}
\frac{d}{dt}N_{00^01} &= 2 \sum_{J(00^01 \rightarrow [10^00,02^00]_{I,II})} (\rho_J E^* + c.c.) \\
\frac{d}{dt}N_{[10^00,02^00]_I} &= -2 \sum_{J(00^01 \rightarrow [10^00,02^00]_I)} (\rho_J E^* + c.c.) \\
\frac{d}{dt}N_{[10^00,02^00]_{II}} &= -2 \sum_{J(00^01 \rightarrow [10^00,02^00]_{II})} (\rho_J E^* + c.c.)
\end{aligned} \tag{4.22}$$

where summation is done over all rotational transitions originating or ending at the corresponding vibrational level. Analogous equations are used for the sequence and the hot bands.

Changes of the average quantum numbers in the vibrational modes due to stimulated transitions are calculated as follows:

$$\begin{aligned}
\Delta e_3 &= \frac{\Delta N_U}{N}, \\
\Delta e_2 &= -2\frac{\Delta N_U}{N} \times \frac{e_2'}{2e_1' + e_2'}
\end{aligned} \tag{4.23}$$

wherein the last term in the second equation takes into account the equilibrium energy distribution between the coupled symmetric stretch and bending vibrations, $e_1' = \frac{1}{\exp\left(\frac{1920}{T_2}\right)-1}$, $e_2' = \frac{2}{\exp\left(\frac{960}{T_2}\right)-1}$, and T_2 is the vibrational temperature before the propagation of the pulse.

New vibrational temperatures are then calculated with Eq. 4.7.

Appendices

Appendix A

Cross-sections of excitation processes

Effective cross-sections are expressed in Å; their numerical values in the nodes are given in the tables below (linear interpolation must be used for determining the values in intermediate points); the data and citations are reproduced from [4].

The following notation for cross-sections is used:
Q_{m1} - Transport cross-section of CO_2 [15];
Q_{m2} - Transport cross-section of N_2 [8];
Q_{m3} - Transport cross-section of He [15];
Q - Cross-section of resonant excitation of N_2 rotation [16, 17];
Q_{11} - Cross-section of the process $(000) \rightarrow (01^10)$ [15];
Q_{12} - Cross-section of the process $(000) \rightarrow (100 + 020)$ [15];
$Q_{13}...Q_{16}$ - Cross-sections of resonant processes around 3.8 eV [15];
Q_{17} - Cross-section of the process $(000) \rightarrow (001)$ [15];
$Q_{18}...Q_{1,10}$ - Cross-sections of electronic excitation and ionization of CO_2 [7];
$Q_{21}...Q_{28}$ - Cross-sections of the process $N_2(v = 0) \rightarrow N_2(v = 1...8)$ [18, 19, 20];
$Q_{29}...Q_{2,15}$ - Cross-sections of electronic excitation and ionization of N_2 [20].

Table A.1: Cross-sections and energies for discharge pumping

u_i	Q_{m1}	u_i	Q_{m2}	u_i	Q_{m3}	u_i	Q
0	140	0	1.4	0	5	0.0015	0
0.04	84	0.001	1.4	0.01	5.4	0.05	0.1
0.1	55	0.002	1.6	0.1	5.8	0.25	0.65
0.3	21	0.008	2	0.2	6.2	0.5	1.15
0.5	10.8	0.01	2.2	1	6.5	0.8	2
0.6	9.4	0.04	4	2	6.1	1	2.65
1	5.7	0.08	6	7	5	1.5	5.6
1.7	5	0.1	6.5	10	4.1	1.8	7.5
2	5.1	0.2	8.8	20	3	1.9	8.2
2.5	6	0.3	9.8			2	8.6
3	7.7	0.4	10			2.15	8.95
4.1	9.4	1	10			2.43	9
5	14.5	1.2	11			2.6	8.9
7.4	10	1.4	12.5			2.75	8.4
10	11.7	1.8	20			2.9	7.65
20	16	2	25			3.25	6.2
27	16.3	2.5	30			3.6	5.1
50	13	3	26			4	4.5
		4	15			4.5	4.16
		5	12			5	3.97
		7	10			5.5	3.93
		10	10			7	4.17
		14	11			9	4.46
		18	12.2			11	4.42
		20	12			15	3.94
		30	10			22	3.15
		100	10			25	3.05

Table A.2: Cross-sections and energies for discharge pumping - continued

u_i	Q_{11}	u_i	Q_{12}	u_i	Q_{13}	u_i	Q_{14}	u_i	Q_{15}
0.083	0	0.167	0	0.252	0	2.37	0	2.37	0
0.085	0.36	0.2	0.54	2.7	0.25	3	0.26	3	0.17
0.09	1.04	0.25	0.82	3	0.4	3.5	0.52	3.65	0.33
0.1	1.6	0.3	0.82	3.3	0.6	4	0.5	3.8	0.31
0.12	1.84	0.5	0.68	3.6	0.65	4.5	0.22	4	0.21
0.14	2.12	0.7	0.56	4.5	0.23	4.6	0.1	4.3	0.1
0.16	2.16	1	0.47	4.6	0.1	5	0	5	0
0.2	2.08	1.4	0.45	5	0				
0.3	1.76	2	0.55						
0.4	1.52	3	1.15						
0.5	1.28	3.9	1.83						
0.6	1.08	4.5	1.4						
0.8	0.8	5	0.4						
1	0.58	6	0.28						
1.2	0.48	10	0.2						
1.6	0.34	20	0.1						
1.8	0.35								
2	0.4								
2.5	0.64								
3	1.04								
3.7	1.4								
4	1.36								
4.2	1.2								
4.5	0.92								
5	0.53								
6	0.4								
8	0.36								
9	0.28								
10	0.16								
10.1	0								
$u_{11} = 0.083$ eV		$u_{12} = 0.167$ eV		$u_{13} = 0.252$ eV		$u_{14} = 0.339$ eV		$u_{15} = 0.422$ eV	

u_i	Q_{16}	u_i	Q_{17}	u_i	Q_{18}	u_i	Q_{19}	u_i	$Q_{1,10}$
2.5	0	0.29	0	7	0	10.5	0	13.8	0
3	0.19	0.3	0.44	8	0.5	11.5	0.56	15	0.1
3.6	0.245	0.35	0.65	8.4	0.6	14	0.8	16	0.13
4	0.21	0.4	0.73	9	0.46	20	1.2	17	0.17
5.07	0	0.5	0.84	10	0.175	30	2	30	1.55
		0.8	1	10.5	0	50	4	40	2.1
		1	1						
		2	0.78						
		6	0.37						
		10	0.25						
		50	0						
$u_{16} = 2.5$ eV		$u_{17} = 0.29$ eV		$u_{18} = 7$ eV		$u_{19} = 10.5$ eV		$u_{1,10} = 13.8$ eV	

Table A.3: Cross-sections and energies for discharge pumping - continued

u_i	Q_{21}	u_i	Q_{22}	u_i	Q_{23}	u_i	Q_{24}	u_i	Q_{25}
0.29	0	1.83	0	1.9	0	2.05	0	2.1	0
0.5	0.0052	1.9	0.208	2	0.416	2.1	0.416	2.15	0.208
0.8	0.0083	2	1.46	2.1	1.33	2.2	1.16	2.2	0.541
1	0.0104	2.05	2.29	2.2	1.87	2.26	1.58	2.3	0.915
1.2	0.0166	2.1	1.66	2.3	1.25	2.55	0	2.46	1.12
1.3	0.0728	2.2	0.79	2.36	0.208	2.75	0.832	2.5	1.12
1.4	0.135	2.35	0.208	2.42	0	2.77	0	2.6	0.208
1.6	0.25	2.45	1.98	2.5	0.499	3	0.208	2.62	0
1.8	0.52	2.5	1.78	2.61	0.915	3.05	0.208	2.68	0
1.9	0.832	2.62	0.208	2.7	0.624	3.25	0	2.8	0.416
2	3.02	2.75	1.04	2.75	0.208			2.9	0.75
2.05	3.12	2.95	1.66	2.8	0			3	0
2.1	2.08	3.05	0.624	2.92	0.416			3.2	0.25
2.15	1.25	3.2	0.208	3	0.208			3.3	0.125
2.2	0.832	3.4	0.208	3.25	0.208			3.35	0
2.3	2.9	4	0	3.31	0				
2.45	1.04								
2.53	1.25								
2.6	1.75								
2.62	2.08								
2.68	1.73								
2.73	0.416								
2.85	0.32								
2.92	0.416								
3.12	0.728								
3.3	0.52								
4	0								
$u_{21} = 0.29$ eV		$u_{22} = 0.58$ eV		$u_{23} = 0.87$ eV		$u_{24} = 1.16$ eV		$u_{25} = 1.45$ eV	

u_i	Q_{26}	u_i	Q_{27}	u_i	Q_{28}	u_i	Q_{29}	u_i	$Q_{2,10}$
2.3	0	2.4	0	2.6	0	5	0	6.8	0
2.4	0.75	2.5	0.208	2.7	0.208	5.9	0.41	7.1	0.57
2.5	1.04	2.75	0.75	2.9	0.29	6.1	0.41	8.1	0.57
2.55	1.12	3	0	3	0.208	7	0.07	8.6	0.25
2.6	1.04	3.2	0.166	3.1	0	9	0	9.5	0.12
2.65	0.624	3.3	0.146	3.2	0			20.7	0
2.7	0.416	3.4	0	3.3	1.04				
2.8	0.208			3.4	0				
2.9	0.125								
3	2.5								
3.1	0.166								
3.2	0								
$u_{26} = 1.74$ eV		$u_{27} = 2.03$ eV		$u_{28} = 2.32$ eV		$u_{29} = 5$ eV		$u_{2,10} = 6.8$ eV	

u_i	$Q_{2,11}$	u_i	$Q_{2,12}$	u_i	$Q_{2,13}$	u_i	$Q_{2,14}$	u_i	$Q_{2,15}$
8.4	0	11.25	0	12.5	0	14	0	15.6	0
8.7	0.42	13.8	0.41	13	0.4	14.3	1.7	18	0.1
9.1	0.42	14	1	13.6	0.4	14.8	1.7	20	0.21
10	0.3	14.7	1	14	0.16	15.6	0.2	50	2.52
20.7	0	15	0.25	20.7	0	20.6	0.2	100	2.52
		65	0			25.4	2.8		
						100	2.8		
$u_{2,11} = 8.4$ eV		$u_{2,12} = 11.25$ eV		$u_{2,13} = 12.5$ eV		$u_{2,14} = 14$ eV		$u_{2,15} = 15.6$ eV	

Appendix B

Molecular constants

The vibrational and rotational constants V and B are listed in Table B.1.

Einstein coefficients A of the laser transitions included in the simulations are summarized in Tables B.2-B.7. Except for the sequence band of *828* isotopologue and the 10-micron transitions of *838* isotopologue, data are taken from the HITRAN2016 database [21] (Einstein coefficients) and our fit of HITRAN data with equation (4.14) (V and B).

For the sequence band of *828* (not included in the HITRAN database), V constants are roughly estimated assuming same shift from *628* as in the regular band, and B constants are assumed to be $\sim$1 % lower than that of regular and hot bands, in analogy with other isotopologues. Einstein coefficients are assumed $\sim$2$\times$ larger than those of the regular band in analogy with other isotopologues.

For the 10-micron transitions of *838* (not included in the HITRAN database), V and B constants are taken from [22]. Einstein coefficients are obtained by scaling the coefficients of the corresponding 9-micron transitions in the assumption that gain coefficients (proportional to transition cross-sections, Eq. 4.15) are roughly the same (according to Freed's measurements [23]).

Table B.1: Molecular constants of CO_2 isotopologues, THz

	626	*628*	*828*	*636*	*638*	*838*
$00^01 \rightarrow [10^00, 02^00]_{I,II}$ ('Regular band')						
$V(00^01 - I)$	28.809	28.969	28.988	27.384	27.692	27.839
$V(00^01 - II)$	31.889	32.158	32.489	30.508	30.610	30.786
$B(00^01)$	0.011589	0.010936	0.010303	0.011593	0.010939	0.010315
$B([10^00, 02^00]_I)$	0.011683	0.011034	0.010403	0.011668	0.011019	0.010403
$B([10^00, 02^00]_{II})$	0.011687	0.011019	0.010375	0.011700	0.011031	0.010394
$00^02 \rightarrow [10^01, 02^01]_{I,II}$ ('Sequence band')						
$V(00^02 - I)$	28.737	28.911	[28.93]	27.300	-	-
$V(00^02 - II)$	31.792	32.029	[32.36]	30.453	-	-
$B(00^02)$	0.011497	0.010859	[0.0103]	0.011512	-	-
$B([10^01, 02^01]_I)$	0.011588	0.010955	[0.0103]	0.011585	-	-
$B([10^01, 02^01]_{II})$	0.011598	0.010946	[0.0103]	0.011623	-	-
$01^{1e}1 \rightarrow [11^{1e}0, 03^{1e}0]_{I,II}$ ('Hot-e band')						
$V(01^{1e}1 - I)$	27.796	27.964	20.190	26.476	26.749	-
$V(01^{1e}1 - II)$	32.124	32.388	32.690	30.689	30.832	-
$B(01^{1e}1)$	0.011602	0.010949	0.010324	0.011605	0.010953	-
$B([11^{1e}0, 03^{1e}0]_I)$	0.011687	0.011036	0.010412	0.011676	0.011028	-
$B([11^{1e}0, 03^{1e}0]_{II})$	0.011695	0.011032	0.010398	0.011702	0.011040	-
$01^{1f}1 \rightarrow [11^{1f}0, 03^{1f}0]_{I,II}$ ('Hot-f band')						
$V(01^{1f}1 - I)$	27.796	27.964	28.019	26.476	26.749	-
$V(01^{1f}1 - II)$	32.124	32.388	32.690	30.689	30.832	-
$B(01^{1f}1)$	0.011620	0.010965	0.010338	0.011623	0.010970	-
$B([11^{1f}0, 03^{1f}0]_I)$	0.011716	0.011063	0.010437	0.011703	0.011053	-
$B([11^{1f}0, 03^{1f}0]_{II})$	0.011723	0.011055	0.010417	0.011733	0.011066	-

Table B.2: Einstein coefficients A of laser transitions of *'626'* CO_2, s^{-1}

	Regular				Sequence				Hot-e				Hot-f			
J	10P	10R	9P	9R	10P	10R	9P	9R	10P	10R	9P	9R	10P	10R	9P	9R
0	-	0.130	-	0.145	-	-	-	-	-	-	-	-	-	-	-	-
1	-	-	-	-	0.809	0.324	0.800	0.322	-	0.106	-	0.130	-	-	-	-
2	0.260	0.168	0.289	0.187	-	-	-	-	-	-	-	-	0.176	0.135	0.216	0.166
3	-	-	-	-	0.484	0.361	0.478	0.359	0.188	0.147	0.230	0.182	-	-	-	-
4	0.222	0.178	0.247	0.199	-	-	-	-	-	-	-	-	0.188	0.155	0.231	0.191
5	-	-	-	-	0.447	0.376	0.442	0.374	0.188	0.159	0.229	0.197	-	-	-	-
6	0.212	0.184	0.235	0.205	-	-	-	-	-	-	-	-	0.186	0.162	0.227	0.201
7	-	-	-	-	0.432	0.384	0.427	0.383	0.185	0.164	0.226	0.204	-	-	-	-
8	0.206	0.186	0.229	0.209	-	-	-	-	-	-	-	-	0.184	0.166	0.225	0.206
9	-	-	-	-	0.423	0.389	0.418	0.389	0.183	0.167	0.223	0.208	-	-	-	-
10	0.203	0.188	0.225	0.212	-	-	-	-	-	-	-	-	0.182	0.169	0.222	0.210
11	-	-	-	-	0.417	0.392	0.413	0.394	0.182	0.169	0.221	0.212	-	-	-	-
12	0.200	0.190	0.223	0.215	-	-	-	-	-	-	-	-	0.180	0.170	0.220	0.212
13	-	-	-	-	0.412	0.395	0.409	0.398	0.180	0.170	0.219	0.214	-	-	-	-
14	0.198	0.191	0.221	0.217	-	-	-	-	-	-	-	-	0.179	0.172	0.219	0.215
15	-	-	-	-	0.408	0.396	0.406	0.401	0.179	0.171	0.217	0.216	-	-	-	-
16	0.196	0.192	0.219	0.218	-	-	-	-	-	-	-	-	0.177	0.172	0.217	0.217
17	-	-	-	-	0.405	0.398	0.403	0.405	0.178	0.171	0.216	0.218	-	-	-	-
18	0.195	0.192	0.218	0.220	-	-	-	-	-	-	-	-	0.176	0.173	0.216	0.218
19	-	-	-	-	0.402	0.399	0.401	0.408	0.177	0.172	0.215	0.220	-	-	-	-
20	0.193	0.192	0.217	0.222	-	-	-	-	-	-	-	-	0.175	0.173	0.215	0.220
21	-	-	-	-	0.399	0.399	0.400	0.411	0.176	0.172	0.214	0.221	-	-	-	-
22	0.192	0.193	0.216	0.223	-	-	-	-	-	-	-	-	0.174	0.174	0.214	0.222
23	-	-	-	-	0.396	0.400	0.398	0.414	0.175	0.172	0.213	0.223	-	-	-	-
24	0.190	0.193	0.215	0.225	-	-	-	-	-	-	-	-	0.173	0.174	0.214	0.223
25	-	-	-	-	0.393	0.400	0.397	0.417	0.175	0.172	0.212	0.224	-	-	-	-
26	0.189	0.193	0.215	0.226	-	-	-	-	-	-	-	-	0.171	0.174	0.213	0.224
27	-	-	-	-	0.390	0.400	0.396	0.420	0.174	0.172	0.211	0.226	-	-	-	-
28	0.188	0.193	0.214	0.228	-	-	-	-	-	-	-	-	0.170	0.174	0.212	0.226
29	-	-	-	-	0.387	0.400	0.395	0.423	0.173	0.172	0.210	0.227	-	-	-	-
30	0.186	0.192	0.214	0.229	-	-	-	-	-	-	-	-	0.169	0.174	0.212	0.227
31	-	-	-	-	0.384	0.399	0.394	0.425	0.172	0.172	0.209	0.229	-	-	-	-
32	0.185	0.192	0.213	0.231	-	-	-	-	-	-	-	-	0.168	0.174	0.211	0.229
33	-	-	-	-	0.381	0.399	0.393	0.428	0.171	0.171	0.208	0.230	-	-	-	-
34	0.183	0.192	0.213	0.232	-	-	-	-	-	-	-	-	0.167	0.173	0.211	0.230
35	-	-	-	-	0.378	0.398	0.393	0.432	0.170	0.171	0.208	0.231	-	-	-	-
36	0.182	0.191	0.212	0.234	-	-	-	-	-	-	-	-	0.166	0.173	0.210	0.231
37	-	-	-	-	0.375	0.397	0.392	0.435	0.169	0.171	0.207	0.233	-	-	-	-
38	0.181	0.191	0.212	0.236	-	-	-	-	-	-	-	-	0.164	0.173	0.210	0.233
39	-	-	-	-	0.372	0.396	0.392	0.438	0.168	0.170	0.207	0.234	-	-	-	-
40	0.179	0.190	0.212	0.237	-	-	-	-	-	-	-	-	0.163	0.172	0.209	0.234
41	-	-	-	-	0.369	0.395	0.392	0.441	0.167	0.170	0.206	0.236	-	-	-	-
42	0.177	0.190	0.212	0.239	-	-	-	-	-	-	-	-	0.162	0.172	0.209	0.236
43	-	-	-	-	0.366	0.393	0.391	0.444	0.166	0.169	0.205	0.237	-	-	-	-
44	0.176	0.189	0.211	0.241	-	-	-	-	-	-	-	-	0.161	0.171	0.209	0.237
45	-	-	-	-	0.363	0.392	0.391	0.447	0.165	0.168	0.205	0.239	-	-	-	-
46	0.174	0.188	0.211	0.242	-	-	-	-	-	-	-	-	0.159	0.171	0.208	0.239
47	-	-	-	-	0.359	0.390	0.391	0.451	0.164	0.168	0.204	0.240	-	-	-	-
48	0.173	0.187	0.211	0.244	-	-	-	-	-	-	-	-	0.158	0.170	0.208	0.240
49	-	-	-	-	0.356	0.388	0.391	0.454	0.163	0.167	0.204	0.241	-	-	-	-
50	0.171	0.186	0.211	0.246	-	-	-	-	-	-	-	-	0.157	0.169	0.208	0.242
51	-	-	-	-	0.352	0.387	0.391	0.458	0.162	0.166	0.203	0.243	-	-	-	-
52	0.169	0.185	0.211	0.248	-	-	-	-	-	-	-	-	0.155	0.168	0.207	0.243
53	-	-	-	-	0.349	0.385	0.391	0.461	0.161	0.165	0.203	0.244	-	-	-	-
54	0.167	0.184	0.211	0.249	-	-	-	-	-	-	-	-	0.154	0.167	0.207	0.245
55	-	-	-	-	0.345	0.382	0.391	0.465	0.160	0.164	0.202	0.246	-	-	-	-
56	0.166	0.183	0.211	0.251	-	-	-	-	-	-	-	-	0.153	0.167	0.207	0.246
57	-	-	-	-	0.342	0.380	0.391	0.468	0.159	0.163	0.202	0.247	-	-	-	-
58	0.164	0.182	0.211	0.253	-	-	-	-	-	-	-	-	0.151	0.166	0.207	0.248
59	-	-	-	-	0.338	0.377	0.392	0.472	0.157	0.162	0.202	0.249	-	-	-	-
60	0.162	-	0.211	-	-	-	-	-	-	-	-	-	0.150	-	0.207	-

Table B.3: Einstein coefficients A of laser transitions of *'628'* CO_2, s^{-1}

	Regular				Sequence				Hot-e				Hot-f			
J	10P	10R	9P	9R	10P	10R	9P	9R	10P	10R	9P	9R	10P	10R	9P	9R
0	-	0.100	-	0.192	-	-	-	-	-	-	-	-	-	-	-	-
1	0.298	0.120	0.574	0.231	-	-	-	-	-	0.089	-	0.162	-	0.089	-	0.162
2	0.199	0.128	0.382	0.248	-	-	-	0.463	0.148	0.113	0.268	0.206	0.148	0.113	0.268	0.206
3	0.179	0.133	0.343	0.257	-	-	0.642	0.481	0.158	0.123	0.285	0.225	0.157	0.124	0.285	0.225
4	0.170	0.136	0.326	0.263	-	0.287	0.611	0.493	0.158	0.129	0.286	0.236	0.158	0.130	0.286	0.236
5	0.165	0.139	0.317	0.268	0.348	0.292	0.593	0.501	0.157	0.133	0.284	0.244	0.157	0.133	0.284	0.243
6	0.162	0.140	0.311	0.271	0.341	0.295	0.581	0.508	0.156	0.136	0.282	0.249	0.156	0.136	0.282	0.248
7	0.159	0.141	0.306	0.274	0.336	0.298	0.573	0.513	0.155	0.137	0.280	0.252	0.155	0.138	0.280	0.252
8	0.158	0.142	0.303	0.276	0.332	0.300	0.567	0.517	0.154	0.139	0.278	0.255	0.154	0.139	0.279	0.255
9	0.156	0.143	0.300	0.278	0.329	0.302	0.562	0.521	0.154	0.140	0.277	0.258	0.153	0.140	0.277	0.257
10	0.155	0.144	0.298	0.280	0.327	0.303	0.558	0.524	0.153	0.141	0.275	0.260	0.152	0.141	0.276	0.259
11	0.154	0.144	0.296	0.282	0.324	0.304	0.555	0.527	0.152	0.141	0.274	0.262	0.151	0.142	0.275	0.261
12	0.153	0.145	0.295	0.283	0.323	0.305	0.552	0.530	0.152	0.142	0.273	0.263	0.151	0.143	0.273	0.263
13	0.152	0.145	0.294	0.284	0.321	0.306	0.549	0.532	0.151	0.142	0.272	0.265	0.150	0.143	0.273	0.264
14	0.152	0.145	0.292	0.285	0.319	0.307	0.547	0.534	0.151	0.143	0.271	0.266	0.150	0.144	0.272	0.265
15	0.151	0.146	0.291	0.287	0.318	0.307	0.545	0.537	0.150	0.143	0.270	0.267	0.149	0.144	0.271	0.267
16	0.150	0.146	0.290	0.288	0.316	0.308	0.543	0.538	0.150	0.143	0.269	0.268	0.149	0.144	0.270	0.268
17	0.150	0.146	0.289	0.289	0.315	0.308	0.542	0.541	0.149	0.143	0.268	0.269	0.148	0.144	0.269	0.269
18	0.149	0.146	0.289	0.290	0.314	0.309	0.540	0.542	0.149	0.144	0.268	0.270	0.148	0.145	0.269	0.270
19	0.148	0.146	0.288	0.291	0.312	0.309	0.539	0.544	0.148	0.144	0.267	0.271	0.147	0.145	0.268	0.271
20	0.148	0.146	0.287	0.291	0.311	0.309	0.538	0.546	0.148	0.144	0.266	0.272	0.147	0.145	0.267	0.272
21	0.147	0.147	0.287	0.292	0.310	0.309	0.537	0.548	0.148	0.144	0.266	0.273	0.146	0.145	0.267	0.272
22	0.147	0.147	0.286	0.293	0.309	0.309	0.535	0.550	0.147	0.144	0.265	0.274	0.146	0.145	0.266	0.273
23	0.146	0.147	0.285	0.294	0.308	0.309	0.534	0.551	0.147	0.144	0.264	0.275	0.145	0.145	0.266	0.274
24	0.146	0.147	0.285	0.295	0.307	0.309	0.533	0.553	0.147	0.144	0.264	0.275	0.145	0.145	0.265	0.275
25	0.145	0.146	0.284	0.296	0.305	0.309	0.532	0.555	0.146	0.144	0.263	0.276	0.144	0.145	0.265	0.276
26	0.144	0.146	0.284	0.297	0.304	0.309	0.532	0.556	0.146	0.144	0.263	0.277	0.144	0.145	0.264	0.276
27	0.144	0.146	0.283	0.298	0.303	0.309	0.531	0.558	0.145	0.144	0.262	0.278	0.143	0.145	0.264	0.277
28	0.143	0.146	0.283	0.298	0.302	0.309	0.530	0.559	0.145	0.144	0.262	0.279	0.143	0.145	0.263	0.278
29	0.143	0.146	0.282	0.299	0.301	0.309	0.529	0.561	0.145	0.144	0.261	0.279	0.142	0.145	0.263	0.279
30	0.142	0.146	0.282	0.300	0.300	0.308	0.528	0.563	0.144	0.144	0.261	0.280	0.142	0.145	0.263	0.280
31	0.142	0.146	0.282	0.301	0.298	0.308	0.528	0.564	0.144	0.143	0.260	0.281	0.141	0.145	0.262	0.280
32	0.141	0.146	0.281	0.302	0.297	0.308	0.527	0.566	0.144	0.143	0.260	0.282	0.141	0.145	0.262	0.281
33	0.141	0.146	0.281	0.302	-	-	0.526	0.568	0.143	0.143	0.259	0.282	0.140	0.145	0.261	0.282
34	0.140	0.145	0.280	0.303	-	-	0.526	0.569	0.143	0.143	0.259	0.283	0.140	0.145	0.261	0.282
35	0.139	0.145	0.280	0.304	-	-	0.525	0.570	0.142	0.143	0.259	0.284	0.139	0.144	0.261	0.283
36	0.139	0.145	0.280	0.305	-	-	0.525	0.572	0.142	0.143	0.258	0.284	0.139	0.144	0.260	0.284
37	0.138	0.145	0.279	0.306	-	-	0.524	0.574	0.142	0.142	0.258	0.285	0.138	0.144	0.260	0.285
38	0.138	0.144	0.279	0.307	-	-	0.523	0.575	0.141	0.142	0.257	0.286	0.138	0.144	0.260	0.286
39	0.137	0.144	0.279	0.307	-	-	0.523	0.577	0.141	0.142	0.257	0.287	0.137	0.144	0.259	0.286
40	0.136	0.144	0.279	0.308	-	-	0.522	0.579	0.140	0.142	0.256	0.287	0.137	0.144	0.259	0.287
41	0.136	0.143	0.278	0.309	-	-	-	-	0.140	0.141	0.256	0.288	0.136	0.143	0.259	0.288
42	0.135	0.143	0.278	0.310	-	-	-	-	0.139	0.141	0.256	0.289	0.136	0.143	0.258	0.288
43	0.134	0.143	0.278	0.311	-	-	-	-	0.139	0.141	0.255	0.290	0.135	0.143	0.258	0.289
44	0.134	0.142	0.277	0.312	-	-	-	-	0.139	0.141	0.255	0.290	0.135	0.143	0.258	0.290
45	0.133	0.142	0.277	0.312	-	-	-	-	0.138	0.140	0.255	0.291	0.134	0.142	0.258	0.291
46	0.133	0.142	0.277	0.313	-	-	-	-	0.138	0.140	0.254	0.292	0.133	0.142	0.257	0.291
47	0.132	0.141	0.277	0.314	-	-	-	-	0.137	0.140	0.254	0.292	0.133	0.142	0.257	0.292
48	0.131	0.141	0.277	0.315	-	-	-	-	0.137	0.139	0.254	0.293	0.132	0.141	0.257	0.293
49	0.131	0.140	0.276	0.316	-	-	-	-	0.136	0.139	0.253	0.294	0.132	0.141	0.257	0.294
50	0.130	0.140	0.276	0.317	-	-	-	-	0.136	0.139	0.253	0.295	0.131	0.141	0.256	0.294
51	0.129	0.140	0.276	0.318	-	-	-	-	0.135	0.138	0.253	0.295	0.131	0.140	0.256	0.295
52	0.128	0.139	0.276	0.318	-	-	-	-	0.135	0.138	0.252	0.296	0.130	0.140	0.256	0.296
53	0.128	0.139	0.276	0.319	-	-	-	-	0.134	0.138	0.252	0.297	0.129	0.140	0.256	0.297
54	0.127	0.138	0.276	0.320	-	-	-	-	0.134	0.137	0.252	0.298	0.129	0.139	0.256	0.297
55	0.126	0.138	0.275	0.321	-	-	-	-	0.133	0.137	0.251	0.298	0.128	0.139	0.255	0.298
56	0.126	0.137	0.275	0.322	-	-	-	-	0.133	0.136	0.251	0.299	0.128	0.138	0.255	0.299
57	0.125	0.137	0.275	0.323	-	-	-	-	0.132	0.136	0.251	0.300	0.127	0.138	0.255	0.300
58	0.124	0.136	0.275	0.324	-	-	-	-	0.132	0.135	0.251	0.301	0.126	0.137	0.255	0.301
59	0.123	0.135	0.275	0.325	-	-	-	-	0.131	0.135	0.250	0.301	0.126	0.137	0.255	0.301
60	0.123	-	0.275	-	-	-	-	-	0.131	-	0.250	-	0.125	-	0.254	-

Table B.4: Einstein coefficients A of laser transitions of *'828'* CO_2, s^{-1}

	Regular				Sequence				Hot-e				Hot-f			
J	10P	10R	9P	9R	10P	10R	9P	9R	10P	10R	9P	9R	10P	10R	9P	9R
0	-	0.073	-	0.234	-	-	-	-	-	-	-	-	-	-	-	-
1	-	-	-	-	[0.2]	[0.2]	[0.7]	[0.7]	-	-	-	0.192	-	-	-	-
2	0.146	0.094	0.466	0.301	-	-	-	-	-	-	-	-	-	-	0.318	0.243
3	-	-	-	-	[0.2]	[0.2]	[0.7]	[0.7]	-	-	0.337	0.267	-	-	-	-
4	0.125	0.100	0.398	0.321	-	-	-	-	-	-	-	-	-	0.105	0.338	0.280
5	-	-	-	-	[0.2]	[0.2]	[0.7]	[0.7]	0.128	0.108	0.336	0.288	-	-	-	-
6	0.119	0.103	0.379	0.330	-	-	-	-	-	-	-	-	0.127	0.111	0.334	0.294
7	-	-	-	-	[0.2]	[0.2]	[0.7]	[0.7]	0.127	0.112	0.332	0.298	-	-	-	-
8	0.116	0.104	0.368	0.337	-	-	-	-	-	-	-	-	0.125	0.113	0.330	0.301
9	-	-	-	-	[0.2]	[0.2]	[0.7]	[0.7]	0.125	0.114	0.328	0.304	-	-	-	-
10	0.114	0.105	0.363	0.340	-	-	-	-	-	-	-	-	0.124	0.115	0.327	0.307
11	-	-	-	-	[0.2]	[0.2]	[0.7]	[0.7]	0.124	0.115	0.325	0.309	-	-	-	-
12	0.112	0.106	0.360	0.343	-	-	-	-	-	-	-	-	0.123	0.116	0.324	0.310
13	-	-	-	-	[0.2]	[0.2]	[0.7]	[0.7]	0.123	0.116	0.322	0.312	-	-	-	-
14	0.111	0.106	0.356	0.347	-	-	-	-	-	-	-	-	0.122	0.117	0.322	0.313
15	-	-	-	-	[0.2]	[0.2]	[0.7]	[0.7]	0.122	0.116	0.320	0.315	-	-	-	-
16	0.110	0.107	0.353	0.349	-	-	-	-	-	-	-	-	0.121	0.117	0.320	0.317
17	-	-	-	-	[0.2]	[0.2]	[0.7]	[0.7]	0.122	0.117	0.318	0.318	-	-	-	-
18	0.109	0.107	0.351	0.351	-	-	-	-	-	-	-	-	0.120	0.118	0.318	0.318
19	-	-	-	-	[0.2]	[0.2]	[0.7]	[0.7]	0.121	0.117	0.317	0.319	-	-	-	-
20	0.108	0.107	0.349	0.353	-	-	-	-	-	-	-	-	0.119	0.118	0.317	0.320
21	-	-	-	-	[0.2]	[0.2]	[0.7]	[0.7]	0.120	0.117	0.315	0.322	-	-	-	-
22	0.108	0.107	0.348	0.355	-	-	-	-	-	-	-	-	0.119	0.118	0.315	0.322
23	-	-	-	-	[0.2]	[0.2]	[0.7]	[0.7]	0.120	0.117	0.314	0.323	-	-	-	-
24	0.107	0.107	0.346	0.357	-	-	-	-	-	-	-	-	0.118	0.118	0.314	0.324
25	-	-	-	-	[0.2]	[0.2]	[0.7]	[0.7]	0.119	0.117	0.312	0.325	-	-	-	-
26	0.106	0.107	0.346	0.359	-	-	-	-	-	-	-	-	0.117	0.118	0.313	0.325
27	-	-	-	-	[0.2]	[0.2]	[0.7]	[0.7]	0.119	0.117	0.311	0.327	-	-	-	-
28	0.105	0.107	0.343	0.360	-	-	-	-	-	-	-	-	0.116	0.118	0.312	0.327
29	-	-	-	-	[0.2]	[0.2]	[0.7]	[0.7]	0.118	0.117	0.310	0.328	-	-	-	-
30	0.105	0.107	0.342	0.362	-	-	-	-	-	-	-	-	0.116	0.118	0.311	0.328
31	-	-	-	-	[0.2]	[0.2]	[0.7]	[0.7]	0.117	0.117	0.309	0.330	-	-	-	-
32	0.104	0.106	0.341	0.364	-	-	-	-	-	-	-	-	0.115	0.118	0.310	0.330
33	-	-	-	-	[0.2]	[0.2]	[0.7]	[0.7]	0.117	0.116	0.307	0.332	-	-	-	-
34	0.103	0.106	0.340	0.365	-	-	-	-	-	-	-	-	0.114	-	0.309	0.332
35	-	-	-	-	[0.2]	[0.2]	[0.7]	[0.7]	-	-	0.307	0.333	-	-	-	-
36	0.102	0.106	0.340	0.367	-	-	-	-	-	-	-	-	-	-	0.308	0.333
37	-	-	-	-	[0.2]	[0.2]	[0.7]	[0.7]	-	-	0.305	0.334	-	-	-	-
38	0.101	0.105	0.339	0.369	-	-	-	-	-	-	-	-	-	-	0.307	0.334
39	-	-	-	-	[0.2]	[0.2]	[0.7]	[0.7]	-	-	0.305	0.336	-	-	-	-
40	0.100	0.104	0.338	0.370	-	-	-	-	-	-	-	-	-	-	0.306	0.336
41	-	-	-	-	[0.2]	[0.2]	[0.7]	[0.7]	-	-	0.304	0.337	-	-	-	-
42	0.100	0.104	0.337	0.372	-	-	-	-	-	-	-	-	-	-	0.305	0.337
43	-	-	-	-	[0.2]	[0.2]	[0.7]	[0.7]	-	-	0.302	0.339	-	-	-	-
44	0.098	0.104	0.336	0.373	-	-	-	-	-	-	-	-	-	-	0.304	0.338
45	-	-	-	-	[0.2]	[0.2]	[0.7]	[0.7]	-	-	0.301	0.340	-	-	-	-
46	0.097	0.103	0.335	0.375	-	-	-	-	-	-	-	-	-	-	0.305	0.342
47	-	-	-	-	[0.2]	[0.2]	[0.7]	[0.7]	-	-	0.300	0.343	-	-	-	-
48	0.096	0.103	0.335	0.376	-	-	-	-	-	-	-	-	-	-	-	-
49	-	-	-	-	[0.2]	[0.2]	[0.7]	[0.7]	-	-	-	-	-	-	-	-
50	0.095	0.102	0.333	0.378	-	-	-	-	-	-	-	-	-	-	-	-
51	-	-	-	-	[0.2]	[0.2]	[0.7]	[0.7]	-	-	-	-	-	-	-	-
52	0.095	0.101	0.333	0.378	-	-	-	-	-	-	-	-	-	-	-	-
53	-	-	-	-	[0.2]	[0.2]	[0.7]	[0.7]	-	-	-	-	-	-	-	-
54	0.093	0.100	0.332	0.381	-	-	-	-	-	-	-	-	-	-	-	-
55	-	-	-	-	[0.2]	[0.2]	[0.7]	[0.7]	-	-	-	-	-	-	-	-
56	0.092	0.099	0.331	0.382	-	-	-	-	-	-	-	-	-	-	-	-
57	-	-	-	-	[0.2]	[0.2]	[0.7]	[0.7]	-	-	-	-	-	-	-	-
58	-	-	0.331	0.384	-	-	-	-	-	-	-	-	-	-	-	-
59	-	-	-	-	[0.2]	[0.2]	[0.7]	[0.7]	-	-	-	-	-	-	-	-
60	-	-	0.331	-	-	-	-	-	-	-	-	-	-	-	-	-

Table B.5: Einstein coefficients A of laser transitions of *'636'* CO_2, s^{-1}

	Regular				Sequence				Hot-e				Hot-f			
J	10P	10R	9P	9R	10P	10R	9P	9R	10P	10R	9P	9R	10P	10R	9P	9R
0	-	0.138	-	0.072	-	-	-	-	-	-	-	-	-	-	-	-
1	-	-	-	-	0.833	0.335	-	0.158	-	0.106	-	0.075	-	-	-	-
2	0.276	0.178	0.143	0.093	-	-	-	-	-	-	-	-	0.175	0.134	0.124	0.095
3	-	-	-	-	0.500	0.374	0.235	0.176	0.188	0.147	0.132	0.105	-	-	-	-
4	0.237	0.190	0.122	0.099	-	-	-	-	-	-	-	-	0.188	0.154	0.132	0.109
5	-	-	-	-	0.462	0.389	0.217	0.184	0.187	0.158	0.131	0.113	-	-	-	-
6	0.225	0.195	0.116	0.102	-	-	-	-	-	-	-	-	0.185	0.162	0.130	0.115
7	-	-	-	-	0.447	0.397	0.209	0.188	0.185	0.164	0.129	0.117	-	-	-	-
8	0.219	0.198	0.113	0.104	-	-	-	-	-	-	-	-	0.183	0.166	0.129	0.118
9	-	-	-	-	0.438	0.403	0.205	0.191	0.183	0.167	0.128	0.120	-	-	-	-
10	0.215	0.200	0.111	0.105	-	-	-	-	-	-	-	-	0.181	0.168	0.127	0.121
11	-	-	-	-	0.431	0.406	0.202	0.194	0.181	0.169	0.126	0.121	-	-	-	-
12	0.213	0.202	0.110	0.107	-	-	-	-	-	-	-	-	0.179	0.171	0.126	0.122
13	-	-	-	-	0.428	0.409	0.200	0.196	0.180	0.170	0.125	0.124	-	-	-	-
14	0.210	0.203	0.109	0.108	-	-	-	-	-	-	-	-	0.179	0.171	0.125	0.123
15	-	-	-	-	0.422	0.413	0.199	0.198	0.179	0.170	0.124	0.125	-	-	-	-
16	0.209	0.204	0.108	0.109	-	-	-	-	-	-	-	-	0.176	0.173	0.125	0.124
17	-	-	-	-	0.419	0.414	0.198	0.200	0.178	0.171	0.124	0.125	-	-	-	-
18	0.207	0.204	0.108	0.110	-	-	-	-	-	-	-	-	0.176	0.173	0.124	0.126
19	-	-	-	-	0.415	0.415	0.197	0.201	0.176	0.172	0.123	0.127	-	-	-	-
20	0.206	0.205	0.107	0.111	-	-	-	-	-	-	-	-	0.174	0.174	0.124	0.127
21	-	-	-	-	0.414	0.416	0.196	0.203	0.177	0.171	0.122	0.128	-	-	-	-
22	0.205	0.206	0.107	0.112	-	-	-	-	-	-	-	-	0.174	0.174	0.123	0.127
23	-	-	-	-	0.411	0.416	0.195	0.205	0.175	0.172	0.121	0.128	-	-	-	-
24	0.203	0.206	0.106	0.112	-	-	-	-	-	-	-	-	0.172	0.174	0.122	0.129
25	-	-	-	-	0.409	0.417	0.195	0.206	0.174	0.172	0.121	0.130	-	-	-	-
26	0.202	0.207	0.106	0.113	-	-	-	-	-	-	-	-	0.171	0.174	0.122	0.130
27	-	-	-	-	0.406	0.418	0.194	0.208	0.174	0.172	0.120	0.131	-	-	-	-
28	0.201	0.207	0.106	0.114	-	-	-	-	-	-	-	-	0.171	0.174	0.122	0.131
29	-	-	-	-	0.403	0.418	0.194	0.210	0.173	0.172	0.120	0.132	-	-	-	-
30	0.199	0.207	0.105	0.114	-	-	-	-	-	-	-	-	0.169	0.175	0.121	0.132
31	-	-	-	-	0.401	0.419	0.193	0.212	0.172	0.172	0.119	0.133	-	-	-	-
32	0.197	0.207	0.105	0.116	-	-	-	-	-	-	-	-	0.169	0.174	0.121	0.132
33	-	-	-	-	0.398	0.419	0.193	0.214	0.171	0.172	0.119	0.134	-	-	-	-
34	0.197	0.206	0.105	0.117	-	-	-	-	-	-	-	-	0.168	0.174	0.121	0.133
35	-	-	-	-	0.396	0.418	0.193	0.215	0.170	0.172	0.118	0.135	-	-	-	-
36	0.196	0.207	0.105	0.118	-	-	-	-	-	-	-	-	0.166	0.174	0.120	0.134
37	-	-	-	-	0.394	0.418	0.193	0.217	0.170	0.171	0.118	0.136	-	-	-	-
38	0.194	0.206	0.105	0.119	-	-	-	-	-	-	-	-	0.165	0.174	0.120	0.135
39	-	-	-	-	0.390	0.419	0.193	0.219	0.169	0.171	0.118	0.136	-	-	-	-
40	0.193	0.206	0.105	0.120	-	-	-	-	-	-	-	-	0.164	0.173	0.120	0.136
41	-	-	-	-	0.389	0.417	0.192	0.220	0.168	0.170	0.117	0.138	-	-	-	-
42	0.192	0.206	0.105	0.121	-	-	-	-	-	-	-	-	0.163	0.173	0.120	0.137
43	-	-	-	-	0.385	0.418	-	-	0.167	0.170	0.117	0.139	-	-	-	-
44	0.190	0.206	0.105	0.122	-	-	-	-	-	-	-	-	0.163	0.173	0.120	0.138
45	-	-	-	-	-	-	-	-	0.166	0.170	0.117	0.139	-	-	-	-
46	0.189	0.205	0.105	0.123	-	-	-	-	-	-	-	-	0.161	0.173	0.120	0.139
47	-	-	-	-	-	-	-	-	0.165	0.169	0.116	0.140	-	-	-	-
48	0.187	0.204	0.105	0.123	-	-	-	-	-	-	-	-	0.160	0.172	0.120	0.140
49	-	-	-	-	-	-	-	-	0.164	0.169	0.116	0.141	-	-	-	-
50	0.186	0.203	0.105	0.125	-	-	-	-	-	-	-	-	0.159	0.172	0.120	0.141
51	-	-	-	-	-	-	-	-	0.163	0.168	0.116	0.142	-	-	-	-
52	0.185	0.203	0.105	0.126	-	-	-	-	-	-	-	-	0.158	0.171	0.119	0.142
53	-	-	-	-	-	-	-	-	0.163	0.167	0.116	0.143	-	-	-	-
54	0.183	0.203	0.105	0.127	-	-	-	-	-	-	-	-	0.157	0.170	0.120	0.143
55	-	-	-	-	-	-	-	-	0.162	0.166	0.116	0.145	-	-	-	-
56	0.182	0.202	0.105	0.128	-	-	-	-	-	-	-	-	0.155	0.170	0.119	0.145
57	-	-	-	-	-	-	-	-	0.161	0.165	0.116	0.146	-	-	-	-
58	0.180	0.201	0.105	0.129	-	-	-	-	-	-	-	-	0.154	0.169	0.119	0.146
59	-	-	-	-	-	-	-	-	0.160	0.165	0.115	0.147	-	-	-	-
60	0.178	-	0.105	-	-	-	-	-	-	-	-	-	0.153	-	0.119	-

Table B.6: Einstein coefficients A of laser transitions of *'638'* CO_2, s^{-1}

	Regular				Sequence				Hot-e				Hot-f			
J	10P	10R	9P	9R	10P	10R	9P	9R	10P	10R	9P	9R	10P	10R	9P	9R
0	-	0.117	-	0.106	-	-	-	-	-	-	-	-	-	-	-	-
1	0.350	0.141	0.315	0.127	-	-	-	-	-	0.093	-	0.098	-	0.093	-	0.098
2	0.233	0.151	0.210	0.136	-	-	-	-	0.155	0.118	0.163	0.125	0.155	0.118	0.163	0.125
3	0.210	0.157	0.189	0.141	-	-	-	-	0.165	0.129	0.173	0.137	0.165	0.130	0.173	0.137
4	0.199	0.160	0.179	0.145	-	-	-	-	0.166	0.136	0.174	0.144	0.165	0.136	0.174	0.144
5	0.194	0.163	0.174	0.147	-	-	-	-	0.165	0.139	0.172	0.148	0.164	0.140	0.173	0.148
6	0.190	0.165	0.171	0.149	-	-	-	-	0.164	0.142	0.171	0.151	0.163	0.142	0.171	0.151
7	0.187	0.166	0.168	0.151	-	-	-	-	0.163	0.144	0.170	0.154	0.162	0.144	0.170	0.153
8	0.185	0.167	0.166	0.152	-	-	-	-	0.162	0.145	0.169	0.155	0.161	0.146	0.169	0.155
9	0.183	0.168	0.165	0.153	-	-	-	-	0.161	0.147	0.168	0.157	0.160	0.147	0.168	0.157
10	0.182	0.169	0.164	0.154	-	-	-	-	0.160	0.147	0.167	0.158	0.159	0.148	0.167	0.158
11	0.181	0.170	0.163	0.155	-	-	-	-	0.159	0.148	0.166	0.159	0.159	0.149	0.167	0.159
12	0.180	0.170	0.162	0.156	-	-	-	-	0.159	0.149	0.166	0.160	0.158	0.150	0.166	0.160
13	0.179	0.171	0.161	0.157	-	-	-	-	0.158	0.149	0.165	0.161	0.157	0.150	0.165	0.161
14	0.178	0.171	0.161	0.158	-	-	-	-	0.158	0.150	0.164	0.162	0.157	0.151	0.165	0.162
15	0.177	0.172	0.160	0.158	-	-	-	-	0.157	0.150	0.164	0.163	0.156	0.151	0.164	0.163
16	0.176	0.172	0.160	0.159	-	-	-	-	0.157	0.150	0.163	0.164	0.156	0.151	0.164	0.163
17	0.176	0.172	0.159	0.160	-	-	-	-	0.156	0.151	0.163	0.164	0.155	0.152	0.164	0.164
18	0.175	0.173	0.159	0.160	-	-	-	-	0.156	0.151	0.162	0.165	0.155	0.152	0.163	0.165
19	0.174	0.173	0.158	0.161	-	-	-	-	0.156	0.151	0.162	0.166	0.154	0.152	0.163	0.165
20	0.174	0.173	0.158	0.161	-	-	-	-	0.155	0.151	0.161	0.166	0.154	0.152	0.162	0.166
21	0.173	0.173	0.158	0.162	-	-	-	-	0.155	0.151	0.161	0.167	0.153	0.153	0.162	0.166
22	0.173	0.173	0.157	0.162	-	-	-	-	0.154	0.151	0.161	0.167	0.153	0.153	0.162	0.167
23	0.172	0.173	0.157	0.163	-	-	-	-	0.154	0.151	0.160	0.168	0.152	0.153	0.161	0.168
24	0.171	0.173	0.157	0.164	-	-	-	-	0.154	0.151	0.160	0.169	0.152	0.153	0.161	0.168
25	0.171	0.173	0.157	0.164	-	-	-	-	0.153	0.151	0.160	0.169	0.151	0.153	0.161	0.169
26	0.170	0.173	0.156	0.165	-	-	-	-	0.153	0.152	0.159	0.170	0.151	0.153	0.161	0.169
27	0.170	0.173	0.156	0.165	-	-	-	-	0.153	0.152	0.159	0.170	0.150	0.153	0.160	0.170
28	0.169	0.173	0.156	0.166	-	-	-	-	0.152	0.151	0.159	0.171	0.150	0.153	0.160	0.170
29	0.168	0.173	0.156	0.166	-	-	-	-	0.152	0.151	0.158	0.171	0.149	0.153	0.160	0.171
30	0.168	0.173	0.156	0.167	-	-	-	-	0.151	0.151	0.158	0.172	0.149	0.153	0.160	0.171
31	0.167	0.173	0.155	0.168	-	-	-	-	0.151	0.151	0.158	0.172	0.148	0.153	0.160	0.172
32	0.167	0.173	0.155	0.168	-	-	-	-	0.151	0.151	0.157	0.173	0.148	0.153	0.159	0.172
33	0.166	0.173	0.155	0.169	-	-	-	-	0.150	0.151	0.157	0.173	0.147	0.153	0.159	0.173
34	0.166	0.173	0.155	0.169	-	-	-	-	0.150	0.151	0.157	0.174	0.147	0.153	0.159	0.173
35	0.165	0.173	0.155	0.170	-	-	-	-	0.149	0.151	0.157	0.175	0.146	0.153	0.159	0.174
36	0.164	0.173	0.155	0.171	-	-	-	-	0.149	0.151	0.157	0.175	0.146	0.153	0.159	0.175
37	0.164	0.173	0.155	0.171	-	-	-	-	0.149	0.151	0.156	0.176	0.146	0.152	0.158	0.175
38	0.163	0.172	0.155	0.172	-	-	-	-	0.148	0.150	0.156	0.176	0.145	0.152	0.158	0.176
39	0.162	0.172	0.155	0.172	-	-	-	-	0.148	0.150	0.156	0.177	0.145	0.152	0.158	0.176
40	0.162	0.172	0.154	0.173	-	-	-	-	0.148	0.150	0.156	0.177	0.144	0.152	0.158	0.177
41	0.161	0.172	0.154	0.174	-	-	-	-	0.147	0.150	0.155	0.178	0.144	0.152	0.158	0.177
42	0.161	0.172	0.154	0.174	-	-	-	-	0.147	0.150	0.155	0.178	0.143	0.152	0.158	0.178
43	0.160	0.171	0.154	0.175	-	-	-	-	0.146	0.149	0.155	0.179	0.142	0.151	0.158	0.178
44	0.159	0.171	0.154	0.175	-	-	-	-	0.146	0.149	0.155	0.179	0.142	0.151	0.158	0.179
45	0.159	0.171	0.154	0.176	-	-	-	-	0.145	0.149	0.155	0.180	0.141	0.151	0.157	0.179
46	0.158	0.170	0.154	0.177	-	-	-	-	0.145	0.149	0.154	0.181	0.141	0.151	0.157	0.180
47	0.157	0.170	0.154	0.177	-	-	-	-	0.145	0.148	0.154	0.181	0.140	0.150	0.157	0.181
48	0.157	0.170	0.154	0.178	-	-	-	-	0.144	0.148	0.154	0.182	0.140	0.150	0.157	0.181
49	0.156	0.169	0.154	0.179	-	-	-	-	0.144	0.148	0.154	0.182	0.139	0.150	0.157	0.182
50	0.155	0.169	0.154	0.179	-	-	-	-	0.143	0.147	0.154	0.183	0.139	0.150	0.157	0.182
51	0.154	0.169	0.154	0.180	-	-	-	-	0.143	0.147	0.154	0.183	0.138	0.149	0.157	0.183
52	0.154	0.168	0.154	0.181	-	-	-	-	0.142	0.147	0.153	0.184	0.138	0.149	0.157	0.184
53	0.153	0.168	0.154	0.181	-	-	-	-	0.142	0.147	0.153	0.184	0.137	0.149	0.157	0.184
54	0.152	0.167	0.154	0.182	-	-	-	-	0.142	0.146	0.153	0.185	0.136	0.148	0.157	0.185
55	0.152	0.167	0.154	0.183	-	-	-	-	0.141	-	0.153	0.186	0.136	-	0.157	0.185
56	0.151	0.167	0.154	0.184	-	-	-	-	-	-	0.153	0.186	-	-	0.157	0.186
57	0.150	0.166	0.154	0.184	-	-	-	-	-	-	0.153	0.187	-	-	0.157	0.187
58	0.149	0.166	0.154	0.185	-	-	-	-	-	-	-	-	-	-	-	-
59	0.149	0.165	0.154	0.186	-	-	-	-	-	-	-	-	-	-	-	-
60	0.148	-	0.155	-	-	-	-	-	-	-	-	-	-	-	-	-

Table B.7: Einstein coefficients A of laser transitions of *'838'* CO_2, s^{-1}

	Regular				Sequence				Hot-e				Hot-f			
J	10P	10R	9P	9R	10P	10R	9P	9R	10P	10R	9P	9R	10P	10R	9P	9R
0	-	-	-	-	-	-	-	-	-	-	-	-	-	-	-	-
1	-	-	-	-	-	-	-	-	-	-	-	-	-	-	-	-
2	-	-	-	-	-	-	-	-	-	-	-	-	-	-	-	-
3	-	-	-	-	-	-	-	-	-	-	-	-	-	-	-	-
4	-	-	-	-	-	-	-	-	-	-	-	-	-	-	-	-
5	-	-	-	-	-	-	-	-	-	-	-	-	-	-	-	-
6	0.191	0.166	0.233	0.203	-	-	-	-	-	-	-	-	-	-	-	-
7	-	-	-	-	-	-	-	-	-	-	-	-	-	-	-	-
8	0.186	0.169	0.227	0.206	-	-	-	-	-	-	-	-	-	-	-	-
9	-	-	-	-	-	-	-	-	-	-	-	-	-	-	-	-
10	0.182	0.171	0.223	0.209	-	-	-	-	-	-	-	-	-	-	-	-
11	-	-	-	-	-	-	-	-	-	-	-	-	-	-	-	-
12	0.180	0.173	0.220	0.211	-	-	-	-	-	-	-	-	-	-	-	-
13	-	-	-	-	-	-	-	-	-	-	-	-	-	-	-	-
14	0.178	0.175	0.219	0.213	-	-	-	-	-	-	-	-	-	-	-	-
15	-	-	-	-	-	-	-	-	-	-	-	-	-	-	-	-
16	0.177	0.177	0.217	0.215	-	-	-	-	-	-	-	-	-	-	-	-
17	-	-	-	-	-	-	-	-	-	-	-	-	-	-	-	-
18	0.176	0.178	0.216	0.217	-	-	-	-	-	-	-	-	-	-	-	-
19	-	-	-	-	-	-	-	-	-	-	-	-	-	-	-	-
20	0.175	0.179	0.215	0.219	-	-	-	-	-	-	-	-	-	-	-	-
21	-	-	-	-	-	-	-	-	-	-	-	-	-	-	-	-
22	0.174	0.180	0.214	0.219	-	-	-	-	-	-	-	-	-	-	-	-
23	-	-	-	-	-	-	-	-	-	-	-	-	-	-	-	-
24	0.174	0.181	0.214	0.221	-	-	-	-	-	-	-	-	-	-	-	-
25	-	-	-	-	-	-	-	-	-	-	-	-	-	-	-	-
26	0.173	0.182	0.213	0.222	-	-	-	-	-	-	-	-	-	-	-	-
27	-	-	-	-	-	-	-	-	-	-	-	-	-	-	-	-
28	0.173	0.184	0.212	0.224	-	-	-	-	-	-	-	-	-	-	-	-
29	-	-	-	-	-	-	-	-	-	-	-	-	-	-	-	-
30	0.172	0.185	0.211	0.225	-	-	-	-	-	-	-	-	-	-	-	-
31	-	-	-	-	-	-	-	-	-	-	-	-	-	-	-	-
32	0.171	0.185	0.210	0.226	-	-	-	-	-	-	-	-	-	-	-	-
33	-	-	-	-	-	-	-	-	-	-	-	-	-	-	-	-
34	-	-	-	-	-	-	-	-	-	-	-	-	-	-	-	-
35	-	-	-	-	-	-	-	-	-	-	-	-	-	-	-	-
36	-	-	-	-	-	-	-	-	-	-	-	-	-	-	-	-
37	-	-	-	-	-	-	-	-	-	-	-	-	-	-	-	-
38	-	-	-	-	-	-	-	-	-	-	-	-	-	-	-	-
39	-	-	-	-	-	-	-	-	-	-	-	-	-	-	-	-
40	-	-	-	-	-	-	-	-	-	-	-	-	-	-	-	-
41	-	-	-	-	-	-	-	-	-	-	-	-	-	-	-	-
42	-	-	-	-	-	-	-	-	-	-	-	-	-	-	-	-
43	-	-	-	-	-	-	-	-	-	-	-	-	-	-	-	-
44	-	-	-	-	-	-	-	-	-	-	-	-	-	-	-	-
45	-	-	-	-	-	-	-	-	-	-	-	-	-	-	-	-
46	-	-	-	-	-	-	-	-	-	-	-	-	-	-	-	-
47	-	-	-	-	-	-	-	-	-	-	-	-	-	-	-	-
48	-	-	-	-	-	-	-	-	-	-	-	-	-	-	-	-
49	-	-	-	-	-	-	-	-	-	-	-	-	-	-	-	-
50	-	-	-	-	-	-	-	-	-	-	-	-	-	-	-	-
51	-	-	-	-	-	-	-	-	-	-	-	-	-	-	-	-
52	-	-	-	-	-	-	-	-	-	-	-	-	-	-	-	-
53	-	-	-	-	-	-	-	-	-	-	-	-	-	-	-	-
54	-	-	-	-	-	-	-	-	-	-	-	-	-	-	-	-
55	-	-	-	-	-	-	-	-	-	-	-	-	-	-	-	-
56	-	-	-	-	-	-	-	-	-	-	-	-	-	-	-	-
57	-	-	-	-	-	-	-	-	-	-	-	-	-	-	-	-
58	-	-	-	-	-	-	-	-	-	-	-	-	-	-	-	-
59	-	-	-	-	-	-	-	-	-	-	-	-	-	-	-	-
60	-	-	-	-	-	-	-	-	-	-	-	-	-	-	-	-

Appendix C

Properties of optical materials

The following expressions and values for linear (n_0) and nonlinear (n_2) refractive indexes and linear absorption (α_0) are used in the program (wavelength λ in the formulas must be expressed in μm):

AgBr

$n_0 = \sqrt{3.860 + \frac{0.8677\lambda^2}{\lambda^2 - 0.3211^2} + \frac{21.61\lambda^2}{\lambda^2 - 254.2^2}}$ (λ = 0.495–12.67 μm) - Fit of data from [24] and [25]

$n_2 = 2.0 \times 10^{-19}$ m^2/W at 9.2 μm - Preliminary data

AgCl

$n_0 = \sqrt{4.00804 + \frac{0.079086}{\lambda^2 - 0.04584} - 0.00085111\lambda^2 - 0.00000019762\lambda^4}$ (λ = 0.578–20.6 μm) [26]

$n_2 = 1.7 \times 10^{-19}$ m^2/W at 9.2 μm - Preliminary data

AMTIR1 (IRG 22)

$n_0 = \sqrt{3.4834 + \frac{2.8203\lambda^2}{\lambda^2 - 0.1352} + \frac{0.9773\lambda^2}{\lambda^2 - 1420.7}}$ (λ = 0.8–15.5 μm) [27]

BaF_2

$n_0 = \sqrt{1.33973 + \frac{0.81070\lambda^2}{\lambda^2 - 0.10065^2} + \frac{0.19652\lambda^2}{\lambda^2 - 29.87^2} + \frac{4.52469\lambda^2}{\lambda^2 - 53.82^2}}$ (λ = 0.15–15 μm) [28]

$n_2 = 1.7 \times 10^{-20}$ m^2/W at 9.2 μm [29]

$\alpha_0 = 0.8(e^{1.20(\lambda - 8)} - 1)$ m^{-1} - Preliminary data

CdTe

$n_0 = \sqrt{1 + \frac{6.1977889\lambda^2}{\lambda^2 - 0.1005326} + \frac{3.2243821\lambda^2}{\lambda^2 - 5279.518}}$ (λ = 6–22 μm) [30]

$n_2 = -2.95 \times 10^{-17}$ m^2/W at 1.06 μm [31]

CsI

$n_0 = \sqrt{1.27587 + \frac{0.68689\lambda^2}{\lambda^2 - 0.130^2} + \frac{0.26090\lambda^2}{\lambda^2 - 0.147^2} + \frac{0.06256\lambda^2}{\lambda^2 - 0.163^2} + \frac{0.06527\lambda^2}{\lambda^2 - 0.177^2} + \frac{0.14991\lambda^2}{\lambda^2 - 0.185^2} + \frac{0.51818\lambda^2}{\lambda^2 - 0.206^2} + \frac{0.01918\lambda^2}{\lambda^2 - 0.218^2} + \frac{3.38229\lambda^2}{\lambda^2 - 161.29^2}}$
($\lambda = 0.25$–67 μm) [32]

$n_2 = 1.2 \times 10^{-19}$ m^2/W - Preliminary data

GaAs

$n_0 = \sqrt{5.372514 + \frac{5.466742\lambda^2}{\lambda^2 - 0.4431307^2} + \frac{0.02429960\lambda^2}{\lambda^2 - 0.8746453^2} + \frac{1.957522\lambda^2}{\lambda^2 - 36.9166^2}}$ ($\lambda = 0.97$–17 μm) [33]

$n_2 = -3.26 \times 10^{-17}$ m^2/W at 1.06 μm [31]

Ge

$n_0 = \sqrt{1 + \frac{0.4886331\lambda^2}{\lambda^2 - 1.393959} + \frac{14.5142535\lambda^2}{\lambda^2 - 0.1626427} + \frac{0.0091224\lambda^2}{\lambda^2 - 752.190}}$ ($\lambda = 2$–14 μm) [34]

$n_2 = 2.83 \times 10^{-17}$ m^2/W at 10.6 μm [31]

KBr

$n_0 = \sqrt{1.39408 + \frac{0.79221\lambda^2}{\lambda^2 - 0.146^2} + \frac{0.01981\lambda^2}{\lambda^2 - 0.173^2} + \frac{0.15587\lambda^2}{\lambda^2 - 0.187^2} + \frac{0.17673\lambda^2}{\lambda^2 - 60.61^2} + \frac{2.06217\lambda^2}{\lambda^2 - 87.72^2}}$ ($\lambda = 0.2$–42 μm) [32]

$n_2 = 4.3 \times 10^{-20}$ m^2/W at 9.2 μm - Preliminary data

KCl

$n_0 = \sqrt{1.26486 + \frac{0.30523\lambda^2}{\lambda^2 - 0.100^2} + \frac{0.41620\lambda^2}{\lambda^2 - 0.131^2} + \frac{0.18870\lambda^2}{\lambda^2 - 0.162^2} + \frac{2.6200\lambda^2}{\lambda^2 - 70.42^2}}$ ($\lambda = 0.18$–35 μm) [32]

$n_2 = 3.4 \times 10^{-20}$ m^2/W at 9.2 μm [29]

NaCl

$n_0 = \sqrt{1.00055 + \frac{0.19800\lambda^2}{\lambda^2 - 0.050^2} + \frac{0.48398\lambda^2}{\lambda^2 - 0.100^2} + \frac{0.38696\lambda^2}{\lambda^2 - 0.128^2} + \frac{0.25998\lambda^2}{\lambda^2 - 0.158^2} + \frac{0.08796\lambda^2}{\lambda^2 - 40.50^2} + \frac{3.17064\lambda^2}{\lambda^2 - 60.98^2} + \frac{0.30038\lambda^2}{\lambda^2 - 120.34^2}}$
($\lambda = 0.2$–30 μm) [32]

$n_2 = 3.5 \times 10^{-20}$ m^2/W at 9.2 μm [29]

NaF

$n_0 = \sqrt{1.0.41572 + \frac{0.32785\lambda^2}{\lambda^2 - 0.117^2} + \frac{3.18248\lambda^2}{\lambda^2 - 40.57^2}}$ ($\lambda = 0.15$–17 μm) [32]

$n_2 = 0.6 \times 10^{-20}$ m^2/W at 9.2 μm - Preliminary data

$\alpha_0 = 5.0(e^{0.97(\lambda - 8)} - 1)$ m^{-1} - Preliminary data

Si

$n_0 = 3.41983 + \frac{0.159906}{\lambda^2 - 0.028} - 0.123109 \left(\frac{1}{\lambda^2 - 0.028}\right)^2 + 1.26878 \times 10^{-6}\lambda^2 - 1.95104 \times 10^{-9}\lambda^4$
($\lambda = 2.44$–25 μm) [35]

$n_2 = 1.0 \times 10^{-17}$ m^2/W at 2.2 μm [36]

SiO_2

$n_0 = \sqrt{1 + \frac{0.6961663\lambda^2}{\lambda^2 - 0.0684043^2} + \frac{0.4079426\lambda^2}{\lambda^2 - 0.1162414^2} + \frac{0.8974794\lambda^2}{\lambda^2 - 9.896161^2}}$ (λ = 0.21–6.7 μm) [37]

$n_2 = 3.29 \times 10^{-20}$ m^2/W at 1.06 μm [31]

ZnS

$n_0 = \sqrt{8.393 + \frac{0.14383}{\lambda^2 - 0.2421^2} + \frac{4430.99}{\lambda^2 - 36.71^2}}$ (λ = 0.405–13 μm) [38]

$n_2 = 2.5 \times 10^{-19}$ m^2/W at 9.2 μm - Preliminary data

ZnSe

$n_0 = \sqrt{1 + \frac{4.45813734\lambda^2}{\lambda^2 - 0.200859853^2} + \frac{0.467216334\lambda^2}{\lambda^2 - 0.391371166^2} + \frac{2.89566290\lambda^2}{\lambda^2 - 47.1362108^2}}$ (λ = 0.54–18.2 μm) [39]
$n_2 = 2.87 \times 10^{-18}$ m^2/W at 1.06 μm [31]

Air

Refractive index n_0 is calculated using Mathar's model for λ = 7.5–14 μm [40]

$n_2 = 3 \times 10^{-23}$ m^2/W at 9.2 μm [41]

Appendix D

Selected formulas explained

Equation 4.4

Eq. 4.4 defines the fraction z_{jk} of discharge energy spent in inelastic collisions:

$$z_{jk} = 10^{16} \frac{y_j u_{jk} \omega_{jk}}{\left(\frac{\xi\mathcal{E}}{\mathcal{N}}\right) v_d}$$

where y_j[-] is the relative concentration of a component in the gas mixture, u_{jk}[eV] is the transferred energy per electron-molecule collision, collision rate constant ω_{jk}[$\mathrm{cm^3 \cdot s^{-1}}$] divided by electron drift speed v_d[$\mathrm{cm \cdot s^{-1}}$] is the collision cross-section ([$\mathrm{cm^2}$]), $\mathcal{E}$[$10^{-16}\mathrm{V \cdot cm^{-1}}$] is the electric field, ξ[$\mathrm{eV \cdot V^{-1}}$] is the energy gained by electron moved across an electric potential difference of 1 V, and $\mathcal{N}$[$\mathrm{cm^{-3}}$] is the total absolute concentration of the gas mixture.

The physical meaning of $\xi\mathcal{E}$ is the energy (in eV) gained by an electron after passing 1 cm in the electric field $\mathcal{E}$. By definition of electronvolt, $\xi = 1$ and is thus omitted in Eq. 4.4.

Pumping rate constants in equations 4.8 and 4.9

Pumping rate constant is the number of quanta added to a given vibrational mode per unit of time per molecule.

$$p_e = \frac{1}{E_v[\mathrm{J}]} \times \frac{1}{N[\mathrm{cm^{-3}}] n[\text{-}] y[\text{-}]} \times q[\text{-}] W[\mathrm{J \cdot s^{-1} \cdot cm^{-3}}]$$

where E_v is the energy of the vibrational quanta: 4.665e-20 J (2349 $\mathrm{cm^{-1}}$) for ν_3 mode of CO_2 (and roughly same for N_2 vibration), and 1.325e-20 J (667 $\mathrm{cm^{-1}}$) for ν_2 mode; N=2.7e19 $\mathrm{cm^{-3}}$ is the density of gas molecules under normal conditions (1 bar, 273 K); q is the fraction of discharge energy deposited in the corresponding vibration; n is the correction factor for molecular density at the conditions different from 'normal'; y is the relative concentration of the gas in the mixture; W is the discharge power density.

Combining the constants and switching to $\mathrm{kW/cm^3}$ for power density and $\mu\mathrm{s^{-1}}$ for the rate constants we get the formulas given in the model description:

$$p_{e4} = 0.8 \times 10^{-3} \frac{q_4}{n y_2} W(t); \quad p_{e3} = 0.8 \times 10^{-3} \frac{q_3}{n y_1} W(t); \quad p_{e2} = 2.8 \times 10^{-3} \frac{q_2}{n y_1} W(t);$$

Bibliography

[1] M. Born and E. Wolf, *Principles of Optics: Electromagnetic Theory of Propagation, Interference and Diffraction of Light*. Cambridge University Press, 1999.

[2] A. E. Siegman, *Lasers*. University Science Books, 1986.

[3] J. Peatross and M. Ware, *Physics of Light and Optics*. Available at optics.byu.edu, 2015.

[4] N. V. Karlov and Y. B. Konev, "High pressure pulsed CO_2 lasers", in *Handbook on lasers*, A. M. Prokhorov, Ed., Moscow: Sovetskoe Radio, 1978 (in Russian).

[5] T. Holstein, "Energy distribution of electrons in high frequency gas discharges", *Phys. Rev.*, vol. 70, pp. 367–384, 1946. DOI: 10.1103/PhysRev.70.367.

[6] W. L. Nighan, "Electron energy distributions and collision rates in electrically excited N_2, CO, and CO_2", *Phys. Rev. A*, vol. 2, pp. 1989–2000, 1970. DOI: 10.1103/PhysRevA.2.1989.

[7] R. D. Hake and A. V. Phelps, "Momentum-transfer and inelastic-collision cross sections for electrons in O_2, CO, and CO_2", *Phys. Rev.*, vol. 158, pp. 70–84, 1967. DOI: 10.1103/PhysRev.158.70.

[8] L. S. Frost and A. V. Phelps, "Rotational excitation and momentum transfer cross sections for electrons in H_2 and N_2 from transport coefficients", *Phys. Rev.*, vol. 127, pp. 1621–1633, 1962. DOI: 10.1103/PhysRev.127.1621.

[9] A. S. Biryukov, V. K. Konyukhov, A. I. Lukovnikov, and R. I. Serikov, "Relaxation of the vibrational energy of the (00^01) level of the CO_2 molecule", *Sov. J. Exp. Theor. Phys.*, vol. 39, p. 610, 1974.

[10] R. L. Taylor and S. Bitterman, "Survey of vibrational relaxation data for processes important in the CO_2-N_2 laser system", *Rev. Mod. Phys.*, vol. 41, pp. 26–47, 1969. DOI: 10.1103/RevModPhys.41.26.

[11] B. J. Feldman, "Short-pulse multiline and multiband energy extraction in high-pressure CO_2-laser amplifiers", *IEEE J. Quant. Electron.*, vol. 9, pp. 1070–1078, 1973. DOI: 10.1109/JQE.1973.1077412.

[12] H. C. Volkin, "Calculation of short-pulse propagation in a large CO_2-laser amplifier", *J. Appl. Phys.*, vol. 50, pp. 1179–1188, 1979. DOI: 10.1063/1.326148.

[13] R. C. Hilborn, "Einstein coefficients, cross sections, f values, dipole moments, and all that", *arXiv:physics/0202029*, 2002.

[14] W. J. Witteman, *The CO_2 Laser*. Berlin Heidelberg New York Tokyo: Springer-Verlag, 1987.

[15] J. J. Lowke, A. V. Phelps, and B. W. Irwin, "Predicted electron transport coefficients and operating characteristics of CO_2-N_2-He laser mixtures", *J. Appl. Phys.*, vol. 44, pp. 4664–4671, 1973. DOI: 10.1063/1.1662017.

[16] Y. D. Oksyuk, "Excitation of the rotational levels of diatomic molecules by electron impact in the adiabatic approximation", *Sov. J. Exp. Theor. Phys.*, vol. 22, pp. 873–881, 1966.

[17] N. Chandra and P. G. Burke, "Rotational excitation cross sections for e^--N_2 scattering", *J. Phys. B: At. Mol. Phys.*, vol. 6, pp. 2355–2357, 1973. DOI: 10.1088/0022-3700/6/11/030.

[18] A. V. Phelps, "Rotational and vibrational excitation of molecules by low-energy electrons", *Rev. Mod. Phys.*, vol. 40, pp. 399–410, 1968. DOI: 10.1103/RevModPhys.40.399.

[19] G. J. Schulz, "Vibrational excitation of nitrogen by electron impact", *Phys. Rev.*, vol. 125, pp. 229–232, 1962. DOI: 10.1103/PhysRev.125.229.

[20] A. G. Engelhardt, A. V. Phelps, and C. G. Risk, "Determination of momentum transfer and inelastic collision cross sections for electrons in nitrogen using transport coefficients", *Phys. Rev.*, vol. 135, A1566–A1574, 1964. DOI: 10.1103/PhysRev.135.A1566.

[21] I. E. Gordon, L. S. Rothman, C. Hill, R. V. Kochanov, Y. Tan, P. F. Bernath, M. Birk, V. Boudon, A. Campargue, K. V. Chance, B. J. Drouin, J.-M. Flaud, R. R. Gamache, J. T. Hodges, D. Jacquemart, V. I. Perevalov, A. Perrin, K. P. Shine, M.-A. H. Smith, J. Tennyson, G. C. Toon, H. Tran, V. G. Tyuterev, A. Barbe, A. G. Császár, V. M. Devi, T. Furtenbacher, J. J. Harrison, J.-M. Hartmann, A. Jolly, T. J. Johnson, T. Karman, I. Kleiner, A. A. Kyuberis, J. Loos, O. M. Lyulin, S. T. Massie, S. N. Mikhailenko, N. Moazzen-Ahmadi, H. S. P. Müller, O. V. Naumenko, A. V. Nikitin, O. L. Polyansky, M. Rey, M. Rotger, S. W. Sharpe, K. Sung, E. Starikova, S. A. Tashkun, J. V. Auwera, G. Wagner, J. Wilzewski, P. Wcisło, S. Yu, and E. J. Zak, "The hitran2016 molecular spectroscopic database", *J. Quant. Spectr. Rad. Transfer*, vol. 203, pp. 3–69, 2017. DOI: 10.1016/j.jqsrt.2017.06.038.

[22] A. Maki, C. Chou, K. Evenson, L. Zink, and J. Shy, "Improved molecular constants and frequencies for the CO_2 laser from new high-j regular and hot-band frequency measurements", *J. Mol. Spectr.*, vol. 167, pp. 211–224, 1994. DOI: 10.1006/jmsp.1994.1227.

[23] C. Freed, "Status of CO_2 isotope lasers and their applications in tunable laser spectroscopy", *IEEE J. Quant. Electron.*, vol. 18, pp. 1220–1228, 1982. DOI: 10.1109/JQE.1982.1071680.

[24] H. Schröer, "Uber die brechungsindizes einiger schwermetallhalogenide im sichtbaren und die berechnung von interpolationsformeln für den dispersionsverlauf", *Z. Phys.*, vol. 67, no. 1-2, pp. 24–36, Jan. 1931. DOI: 10.1007/bf01391040. [Online]. Available: https://doi.org/10.1007/bf01391040.

[25] D. E. McCarthy, "Refractive index measurements of silver bromide in the infrared", *Appl. Opt.*, vol. 12, no. 2, p. 409, Feb. 1973. DOI: 10.1364/ao.12.000409. [Online]. Available: https://doi.org/10.1364/ao.12.000409.

[26] L. W. Tilton, E. K. Plyler, and R. E. Stephens, "Refractive index of silver chloride for visible and infrared radiant energy", *J. Opt. Soc. Am.*, vol. 40, no. 8, p. 540, Aug. 1950. DOI: 10.1364/josa.40.000540. [Online]. Available: https://doi.org/10.1364/josa.40.000540.

[27] *SCHOTT IRG 22 product flyer*, Apr. 2017. [Online]. Available: https://refractiveindex.info/download/data/2017/schott-infrared-chalcogenide-glasses-irg-22-english-us-11052017.pdf.

[28] H. H. Li, "Refractive index of alkaline earth halides and its wavelength and temperature derivatives", *J. Phys. Chem. Ref. Data*, vol. 9, no. 1, pp. 161–290, Jan. 1980. DOI: 10.1063/1.555616. [Online]. Available: https://doi.org/10.1063/1.555616.

[29] M. N. Polyanskiy, I. V. Pogorelsky, M. Babzien, R. Kupfer, K. L. Vodopyanov, and M. A. Palmer, "Post-compression of long-wave infrared 2 picosecond sub-terawatt pulses in bulk materials", *Opt. Express*, vol. 29, no. 20, p. 31 714, Sep. 2021. DOI: 10.1364/oe.434238.

[30] A. G. DeBell, E. L. Dereniak, J. Harvey, J. P. J. Nissley, A. Selvarajan, and W. L. Wolfe, "Cryogenic refractive indices and temperature coefficients of cadmium telluride from 6 μm to 22 μm", *Appl. Opt.*, vol. 18, pp. 3114–3115, 1979. DOI: 10.1364/AO.18.003114.

[31] M. Sheik-Bahae, "Dispersion of bound electron nonlinear refraction in solids", *IEEE J. Quant. Electron.*, vol. 27, pp. 1296–1309, 1991. DOI: 10.1109/3.89946.

[32] H. H. Li, "Refractive index of alkali halides and its wavelength and temperature derivatives", *J. Phys. Chem. Ref. Data*, vol. 5, pp. 329–528, 1976. DOI: 10.1063/1.555536.

[33] T. Skauli, P. S. Kuo, K. L. Vodopyanov, T. J. Pinguet, O. Levi, L. A. Eyres, J. S. Harris, M. M. Fejer, L. B. B. Gerard, and E. Lallier, "Improved dispersion relations for GaAs and applications to nonlinear optics", *J. Appl. Opt.*, vol. 94, pp. 6447–6455, 2003. DOI: 10.1063/1.1621740.

[34] J. H. Burnett, S. G. Kaplan, E. Stover, and A. Phenis, "Refractive index measurements of ge", P. D. LeVan, A. K. Sood, P. Wijewarnasuriya, and A. I. D'Souza, Eds., SPIE Optical Engineering + Applications, 2016, San Diego, California, United States, SPIE, Sep. 2016. DOI: 10.1117/12.2237978. [Online]. Available: https://doi.org/10.1117/12.2237978.

[35] D. F. Edwards and E. Ochoa, "Infrared refractive index of silicon", *Appl. Opt.*, vol. 19, pp. 4130–4131, 1980. DOI: 10.1364/AO.19.004130.

[36] A. D. Bristow, N. Rotenberg, and H. M. van Driel, "Two-photon absorption and kerr coefficients of silicon for 850–2200 nm", *Appl. Phys. Lett.*, vol. 90, p. 191 104, 2007. DOI: 10.1063/1.2737359.

[37] I. H. Malitson, "Interspecimen comparison of the refractive index of fused silica$*, y$", *J. Opt. Soc. Am.*, vol. 55, no. 10, p. 1205, Oct. 1965. DOI: 10.1364/josa.55.001205. [Online]. Available: https://doi.org/10.1364/josa.55.001205.

[38] C. A. Klein, "Room-temperature dispersion equations for cubic zinc sulfide", *Appl. Opt.*, vol. 25, no. 12, p. 1873, Jun. 1986. DOI: 10.1364/ao.25.001873. [Online]. Available: https://doi.org/10.1364/ao.25.001873.

[39] B. Tatian, "Fitting refractive-index data with the Sellmeier dispersion formula", *Appl. Opt.*, vol. 23, pp. 4477–4485, 1984. DOI: 10.1364/AO.23.004477.

[40] R. J. Mathar, "Refractive index of humid air in the infrared: Model fits", *J. Opt. A*, vol. 9, pp. 470–476, 2007. DOI: 10.1088/1464-4258/9/5/008.

[41] M. N. Polyanskiy, M. Babzien, I. V. Pogorelsky, R. Kupfer, K. L. Vodopyanov, and M. A. Palmer, "Single-shot measurement of the nonlinear refractive index of air at 92 μm with a picosecond terawatt CO2 laser", *Opt. Lett.*, vol. 46, no. 9, p. 2067, Apr. 2021. DOI: 10.1364/ol.423800.